KU LEUVEN

FACULTY OF ENGINEERING TECHNOLOGY

TECHNOLOGYCAMPUS BRUGGE

Improvements on Design and Analysis of Deep Beams Based on the Strut-and-Tie Method

(FECHA DEFENSA: 21 /06/ 2018)

MÁSTER EN EDIFICACIÓN

MODALIDAD DE INTERCAMBIO ACADÉMICOS, ESTUDIANTES RECIBIDOS

TRABAJO FIN DE GRADO - CURSO 2017-18

AUTOR:

TIJS VANCOILLIE

TUTOR ACADÉMICO UPV:

Enrique David Llacer

UNIVERSITAT POLITÈCNICA DE VALÈNCIA

ESCOLA TÈCNICA SUPERIOR ENGINYERIA D'EDIFICACIÓ

ETS d'Enginyeria d'Edificació
Universitat Politècnica de València

Academic Year 2017-2018

FACULTEIT INDUSTRIELE INGENIEURSWETENSCHAPPEN
TECHNOLOGIECAMPUS OOSTENDE
Spoorwegstraat 12
8200 BRUGGE, België
tel. + 32 50 66 48 00
iiw.brugge@kuleuven.be
www.iiw.kuleuven.be

Master Thesis submitted to obtain the degree of Master of Science in Engineering Technology

Academic year 2017 – 2018

by

Tijs Vancoillie

Summary:

The strut-and-tie method is an alternative design and analysis method for discontinuity regions like deep beams and pile caps. In the following Master's Thesis, the method is entirely explained using guidelines from ACI. In a second part, the expansion of the method towards the design and analysis of deep beams is investigated with a critical analysis. A list of improvements is presented and discussed.

Foreword/Resignation

As a last year master's student in Engineering at the KU Leuven University, I took part in the Erasmus exchange program and went to Valencia to study at the Universitat Politècnica de València. There I had the opportunity to write my Master's Thesis during semester B in English. Because of the preliminary background knowledge that was obtained through courses at the home university, I chose the subject on the strut-and-tie model. This model is an innovative method that still has some improvements to make, which convinced me to work on it.

This Master's Thesis was written together with fellow Belgian student Anthony Demeyere, who also took part of the Erasmus exchange. To gather the prior knowledge on the strut-and-tie method, we performed a literature study together in the form of a state of the art. Later, two specific subjects were further examined and this thesis represents one of them. Both of us worked together on all parts, this way we could help each other whenever needed.

We would like to thank both the KU Leuven University and the Universitat Politècnica de València for the opportunity and the cooperation, professors Marc Spegelaere (KUL) and Peter Minne (KUL) who provided us with the necessary background knowledge to understand this topic on concrete calculations and behaviour and Enrique David Llacer (UPV) for guiding us during the entire process and research on the strut-and-tie method. I also want to thank my parents who supported and helped me throughout my four years of studying and during my work for the Master Thesis. Another thank you to my girlfriend for always supporting me mentally during these last couple of months.

Tijs Vancoillie

Table of contents

1 Introduction

The strut-and-tie method is a simplified method to analyse and design reinforced concrete structures. The STM is used to design the discontinuity-regions, where the rules of Bernouillie don't satisfy anymore. Examples of such regions are pile caps, corbels, deep beams, etc. Generally these are all the places with a disturbed geometry or in regions with discontinuity of loads. The main principle is that loads are carried through the concrete until they reach a supporting point. The model is based on drawing traces of the stresses on the structure and dividing the structure into connected struts, ties and nodes.

The STM for bidimensional problems like deep beams and corbels has already been thoroughly investigated in recent years and is very well known today but it's still not perfect. The strength of deep beams is controlled by shear rather than by flexure. Shear behaviour in deep beams, and generally reinforced concrete elements, is still not well known. Shear depends on many parameters, but existing models rely on empirical equations. Therefore these parameters, that are influencing the shear behaviour, need to be further investigated. Also the strut efficiency factor was further investigated.

The purpose of this Master's Thesis is to investigate the most recent insights and research works on applying the strut-and-tie method to predict shear behaviour of deep beams. Also some research was done towards the strut efficiency factor.

In a first part, the method is generally explained in the form of a state of the art. The different elements of the STM and design steps according to ACI are illustrated. This knowledge was needed to understand the researched papers.

The next step is to investigate which STM-based approaches for deep beams that have been proposed so far. The aim of this Master's Thesis is to provide the readers with a table of improvements and proposals throughout the years. The essentials of each researched paper are explained and discussed in a critical analysis.

As a conclusion of this study, suggestions are presented on what approaches and improvements could be the most reliable or interesting for the design and analysis of deep beams using the strut-and-tie method.

2 Strut-and-Tie method

2.1 History

Structures have been built since the old ages composing of wood, brick, stone and even concrete. The use of concrete dates back several centuries, in the time of the Romans, the middle ages. The real driver for the use of concrete was the Smeaton's tower in the years 1756 to 1759. The engineer John Smeaton first used hydraulic lime in concrete, using pebbles and powdered brick as aggregate. In the late 19th century Joseph Monier pioneered with the introduction of using steel in combination with concrete because the concrete containers he made, weren't strong enough. The use of steel in concrete as we know today, is to overcome the low tensile strength of concrete. With the introduction of reinforced concrete, structures could be built with a good compressive and tensile strength.

It's only in the year 1899, when reinforced concrete was still in its infancy, that a researcher developed a model for designing reinforced concrete. This first model was called a truss model and was introduced by Wilhelm Ritter (1899). The truss model was used for the visualization of internal forces, compression and tension, in the structural element and to define the amount of reinforcement. The model describes that tensile forces would be carried by steel rods (ties) and compressive forces would be carried by the concrete (struts), as can be seen in figure 1. In 1902 the researcher Emil Mörsch took Ritter's work and refined his model. Ritter used discrete diagonal forces but Mörsch refined this observation by saying that the forces are in a continuous field of diagonal compression. The adaptation to Ritter's model can be seen in figure 2.

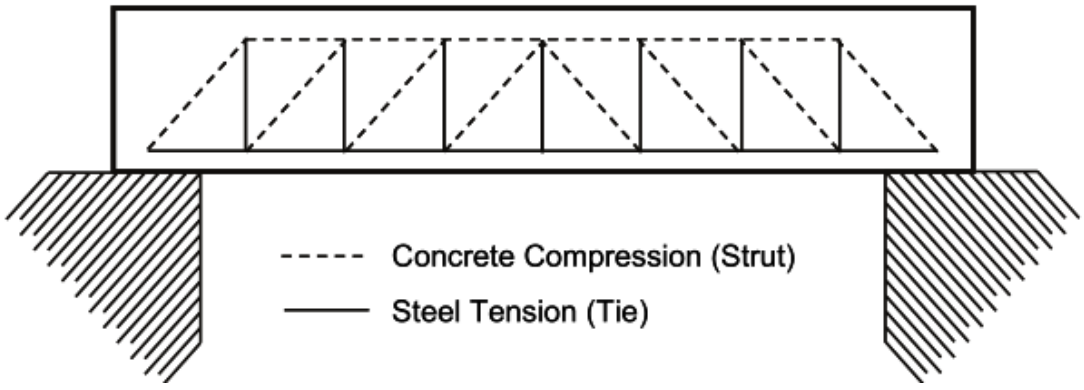

Figure 1: Ritter's original truss analogy (Brown, 2005)

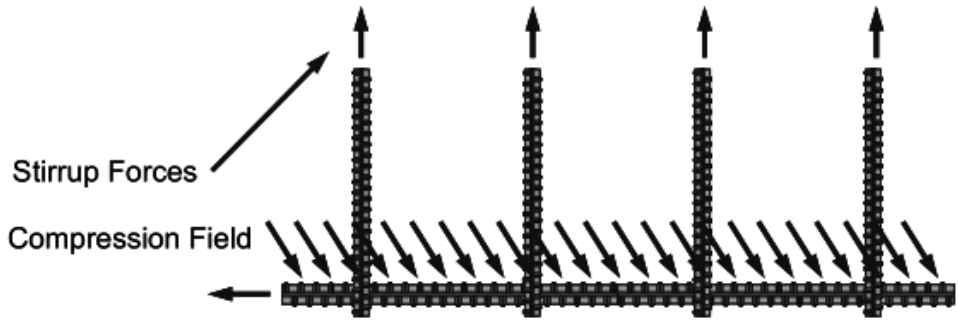

Figure 2: Mörsch's adaptation of Ritter's model (Brown, 2005)

This model was further researched by Talbot (1909) and Richart (1927). They studied the effects of shear on the reinforced concrete elements. Talbot discovered that the truss models made overestimations considering the strength of the concrete element. This was due to the neglection of the tensile strength in the truss model. But the tensile strength of concrete is an important factor when it comes to shear resistance in reinforced concrete elements. Richart further researched this and developed a method of shear design. This method took both steel and concrete contributions into consideration when calculating the shear resistance of the element. The shear resistance was determined by calculating the concrete and steel contribution to shear strength separately and then make the sum of both (V_c+V_s). This method can still be found in the sectional approach.

In the year 1964, Kupfer (1964) expanded the Morsch's truss analogy by the application of the principle of minimum strain energy. Shortly after, in the year 1965, Kupfer studied the shear reinforcement in concrete beams and slabs and suggested a simple method to reduce the shear reinforcement in those concrete elements.

It was until the early 1970s that the truss analogy or the now called strut-and-tie method was really revived in the United States. At that time, a strut-and-tie model was applied for the first time to concrete elements subjected to both shear and torsion. Lambert & Thurlimann (1971) developed an instrument to assess these kind of cases. This instrument consisted of a tubular truss that formed a hollow box around the concrete elements' outside face (figure 3). This was actually a reinforcing cage, consisting of longitudinal reinforcement, stirrups and concrete compression diagonals.

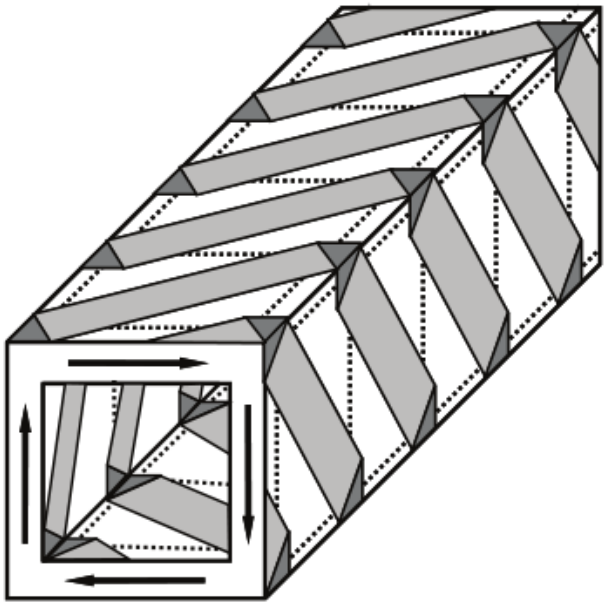

Figure 3: Tubular truss (Brown, 2005)

This tubular truss was then further refined to a space truss model by the following references (Lüchinger, 1977), (Ramirez & Breen, 1983) and (Collins & Mitchell, 1986). The refined space truss model could account for bending, shear, torsion and axial load.

Because of the increasing interest in the strut-and-tie modelling, researchers started to publish general methods for the application of the strut-and-tie model for use in discontinuity regions (Marti, 1985a), (Marti, 1985b) and (Schlaich, Schäfer, & Jennewein, 1987). Because of these proposed approaches it became widely accepted and applicable to all kinds of structures. The strut-and-tie method became an effective method to design elements with load discontinuities or geometric changes. The proposed approaches included basic tools that could be applied to complex structures so they could safely design structures using behavioral models. This was seen as the first step towards an unified design method for concrete structures (Williams, Deschenes, & Bayrak, 2012).

Because of this unified design, the strut-and-tie method could be adopted and used in many codes around the world. First of all, it was adapted in the Canadian CSA standard in the year 1984. Later on, it was implemented in the American Association of State Highway and Transportation Officials (AASHTO) in 1989 for the segmental guide specifications and in 1994 for bridge design specifications. In 2002, the American Concrete Institute (ACI) included the strut-and-tie method in the building code requirements for structural concrete (ACI Comittee 318, 2002). Macgregor in the year 2002 published a special publication (SP-208) with information about the background of provisions included into the ACI code. Nowadays most

countries have the strut-and-tie method incorporated into their design codes for concrete structures. (Martin & Sanders, 2007), (Brown, 2005)

2.2 Main principles

In the design of structural concrete there are two limit states that can be considered. The first one is the ultimate limit state (ULS). When designing according to these rules, members are designed for strengths until ultimate failure loads and failing of the structure. Safety factors are then applied to remain conservative. The second one is the serviceability limit state (SLS). This limit state considers serviceability characteristics such as cracks, deflections, deformations etc. Logically, lower maximum strength values are obtained for a same member in this state because these considered phenomena appear before failure.

The STM is a method to design and calculate concrete members in the ultimate limit state. The concrete members are designed to resist a specific ultimate force until failure. Consequently experimental tests conducted to check the STM predictions are applied on the members until failure.

The Strut-and-Tie method is based on the lower bound theorem. The external loads are assumed to be transferred through the concrete mass by internal stresses in the different materials. A model is chosen to represent these stress paths and consequently the internal stress can be calculated in each point of the model. If these stresses, derived from the geometry and external loads, are smaller than the maximum failure loads at each point, then failure will not occur.

2.3 Elements of the STM

To discuss the elements of the strut-and-tie model a combination of following works was used: (Martin & Sanders, 2007), (Brown, 2005), (Williams et al., 2012), (ACI Comittee 318, 2002).

Strut-and-tie modeling is used to design discontinuity regions, also called D-regions, in reinforced concrete structures. The objective of STM is to reduce to level of stress in these D-regions due to the influence of exterior forces. By using STM the complex states of stress within the elements are reduced into a truss existing of simple states of stress. These are uniaxial stress paths. Each of these simple uniaxial stress paths are parts of the STM model. A strut-

and-tie model exists of three elements: struts, ties and nodes (figure 4). The forces in these elements need to be known and can be calculated using the simple truss geometry. Once these forces are known, the resulting stresses in the elements are also known. These can then be compared with the codes if it's permissible. Because of the uniaxial tension and compression within the element, the appropriate reinforcement (in the form of steel bars, meshes, etc.) is essential.

In the strut-and-tie model you have three major components as mentioned above: struts, ties and nodes.

- Struts: The elements of the STM that represents the compressive stresses.
- Ties: The elements of the STM that represents the tensile stresses.
- Nodes/nodal zones: The elements of the STM where the struts and ties are connected.

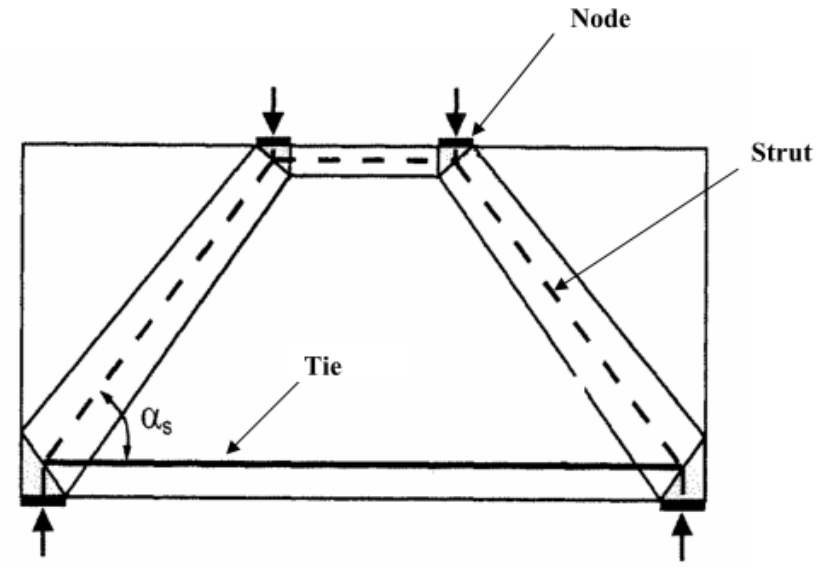

Figure 4: The elements of the strut-and-tie model (Martin & Sanders, 2007)

2.3.1 Struts

Struts are the elements of the STM that represents the compressive stresses in the concrete structure. These struts transfer the forces from the loads on the element to the supports of the element. Struts varies widely in geometry, depending on the specific force path that arises from each single strut. Even if these struts varies widely, three major geometric shape groups can be found for struts. These are prismatic, bottle shaped and compression fan shaped struts. The struts shapes are illustrated in figure 5 for deep beams.

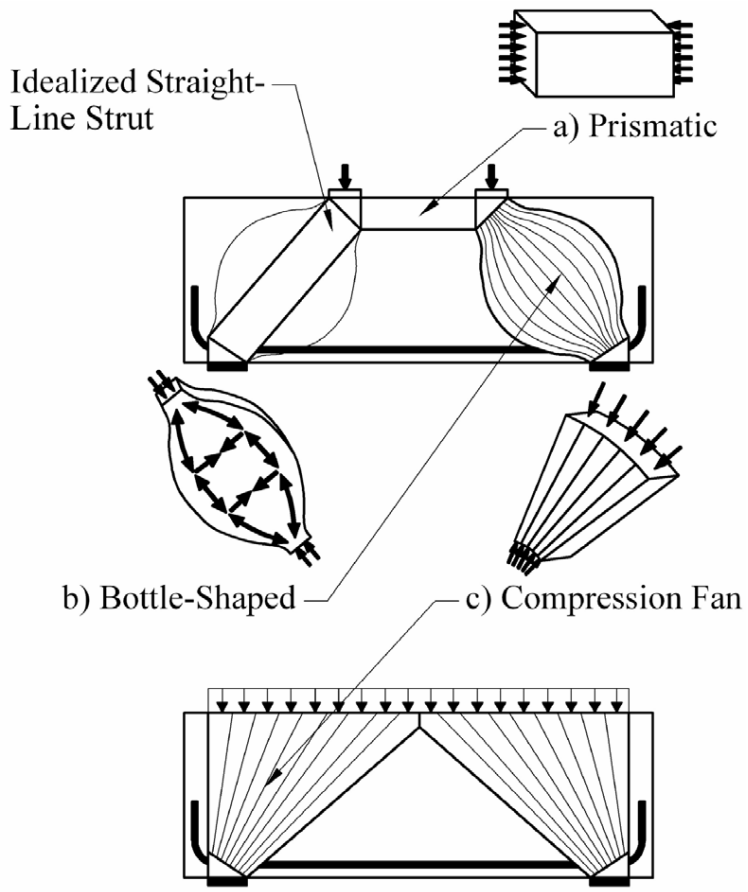

Figure 5: Different types of struts (Martin & Sanders, 2007)

Prismatic shaped struts are the most basic ones. They can be found where the loads on the element are uniform, therefore the stresses are uniform. Because of the uniform loads on this specific strut, the cross section of the struts are also uniform. As shown in figure 5 these kind of struts are located in the compression area at the top of the deep beam if there is positive bending.

Bottle shaped struts are formed when the geometrical conditions at the ends of the strut are well known but in the middle of the strut are not confined to a part of an element. This means that they're located in a part of an element where the middle of the strut can spread out. Forces applied to the ends of these struts lead to compression stresses. As the compression stresses disperse from both ends, they change direction and create an angle. Therefore forming a bottle shaped strut as shown in figure 5. The spreading of the stresses are not desirable because this leads to tension fields at the place of dispersion. For bottle shaped struts, designers should consider ties to represent these tensile forces as shown in figure 6. The bottle shaped struts can be simplified into prismatic shaped struts. Transverse reinforcement is then needed to counter the transverse tension. If the tensile stresses in the bottle shaped struts are too big,

the occurrence of cracks in the concrete element is possible. The cracking in the strut has been researched by Sclaich et al. (1987) and Reineck (2002). The research concluded that this type of cracking occurs when compressive stresses exceeds 0,55 f_c' at the end of bottle shaped struts.

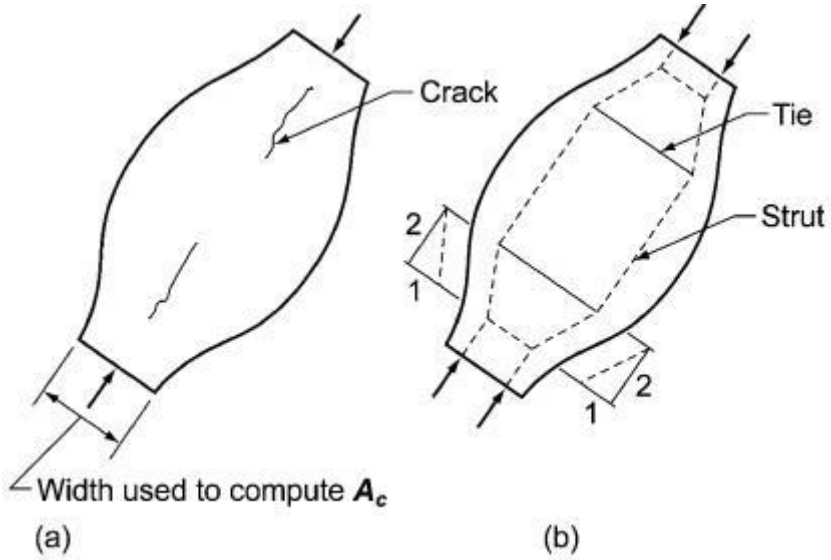

Figure 6: Bottle-shaped strut (ACI Comittee 318, 2002)

Compression fan shaped struts are formed when stresses from a bigger area flow to a smaller area as shown in figure 5. Stresses are focused on a small area. These kind of struts have zero to none curvature and consequently they don't develop transverse tensile stresses. A simple example of a compression fan strut is a strut that transports a uniform load to a support point.

Struts can fail duo to:

- The cracking/splitting of struts
- The buckling of struts
- Compression failure of the concrete
- Bursting of struts due to transverse tension

2.3.2 Ties

Ties are the elements of the STM that represent the tensile stresses in the concrete structure and represent the equivalent tensile forces. As known concrete has a small tensile capacity, which is around 10% of the compression capacity. But this tensile capacity of concrete is in

most cases neglected because of strength concerns. A tie consists of steel reinforcement rebars and a hypothetical prism of concrete around the reinforcement bar. Because only the steel reinforcement bar contributes to the tensile resistance, it's easier to determine the geometry and capacity of the tie. The capacity of the tie depends on the yield strength of the steel. The ties geometry will be the same as the steel reinforcement bar, hereby it's important that the steel reinforcement bar is placed so that the centroid of the reinforcement coincides with the axis of the tie. The area of the steel reinforcement bar A_{st} can be calculated with the following equation: (ACI Comittee 318, 2002)

$$A_{st} = \frac{F_u}{\emptyset f_y}$$

F_u is the force in the tie, f_y is the yield strength of the steel and $\emptyset$ is a reduction factor.

The anchorage of the ties are also important. The anchorage needs to be provided beyond the point that the yield force of the tie is expected, which will be further explained more into detail.

Struts can fail due to:

- Insufficient end anchorage
- Lacking of reinforcement quantity

2.3.3 Nodes

Nodes/nodal zones are the elements of the STM where the struts and ties are connected. First of all the difference between nodes and nodal zones. The point where the struts, ties and forces of the struts and ties intersect are the nodes. The area of concrete around these nodes are the nodal zones (figure 7). Three forces always have to act on the node otherwise the equilibrium of vertical and horizontal forces is not in balance. Calculations are made easier by dividing the reaction force into two forces (R => R_1, R_2).

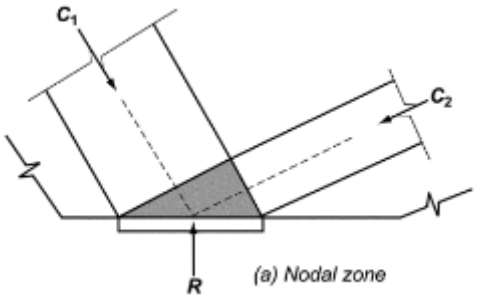

Figure 7: The representation of a nodal zone. (ACI Comittee 318, 2002)

Nodes are described by the elements, thereby the forces, acting on the node. Three major node types can be found: C-C-C nodes, C-C-T nodes and C-T-T nodes, these can be seen in figure 8. C-C-C nodes are nodes where only struts intersects. C-C-T nodes are nodes where there is only one tie that is intersecting with struts. C-T-T nodes are nodes where there are more than two ties and only one strut intersecting. There is also a fourth option T-T-T nodes where only ties intersect, however most design specifications don't identify these kind of nodes (figure 9). The geometry of nodal zones are based on the bearing conditions, the details of anchored reinforcement and the geometry of struts and ties intersecting in the node. As known, concrete has a great compression capacity therefore the C-C-C nodes has the greater concrete efficiency, bigger strength, of all the types of nodes.

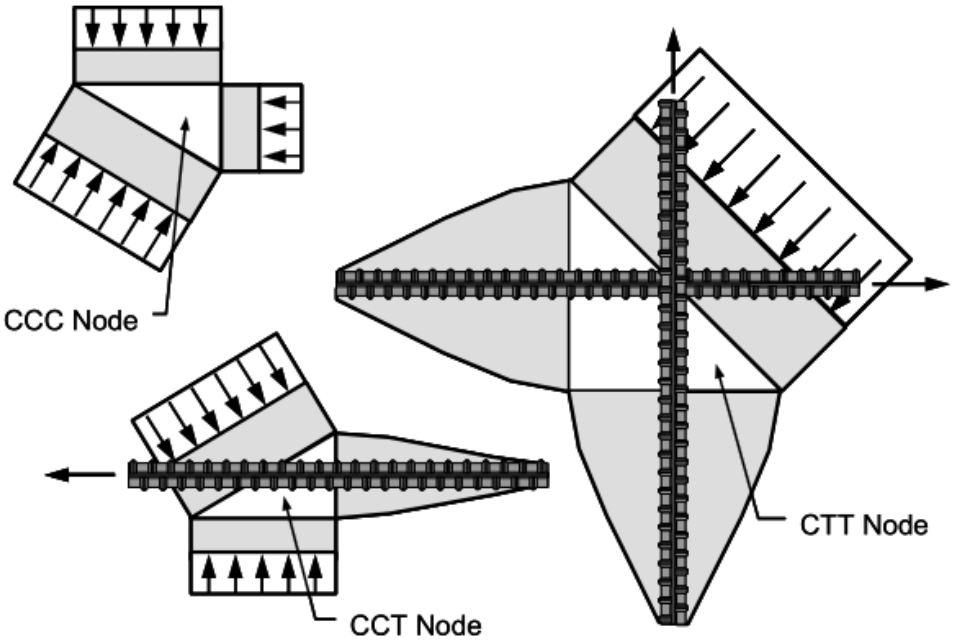

Figure 8: The different types of nodes. (Brown, 2005), (ACI Comittee 318, 2002)

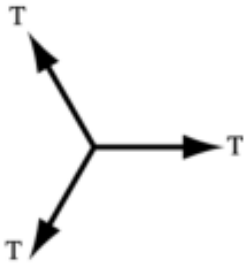

Figure 9: T-TT node

There are three major types of nodes, but each type of node can be detailed as a hydrostatic node or a non-hydrostatic node (figure 10). In hydrostatic nodes, the stress on each side of the node is equal and perpendicular to the face of the node. Because of the fact that the stresses are perpendicular to the faces of the nodes, there is no presence of shear stresses on the faces of the nodes. Successfully achieving hydrostatic nodes in STM is almost not possible and most of the time non-viable. Because of the impossibility and impracticality, STM uses non-hydrostatic nodes. When the node is non-hydrostatic, the stresses aren't equal and perpendicular to the faces of the node. Instead of equal stresses, they are proportioned based upon the stresses on the node. Schlaich et al. (1987) stated that for non-hydrostatic nodes the ratio of the maximum stress on a side of the node to the minimum stress on a side of the node needed to be lower than two. The different states of stress in both hydrostatic as non-hydrostatic nodes is shown in figure 10.

The size of a hydrostatic node can be determined using the stress and force on the node. Based on figure 10, the next equation can be utilized to determine the size:

$$w_1 = \frac{F_1}{\sigma_1}$$

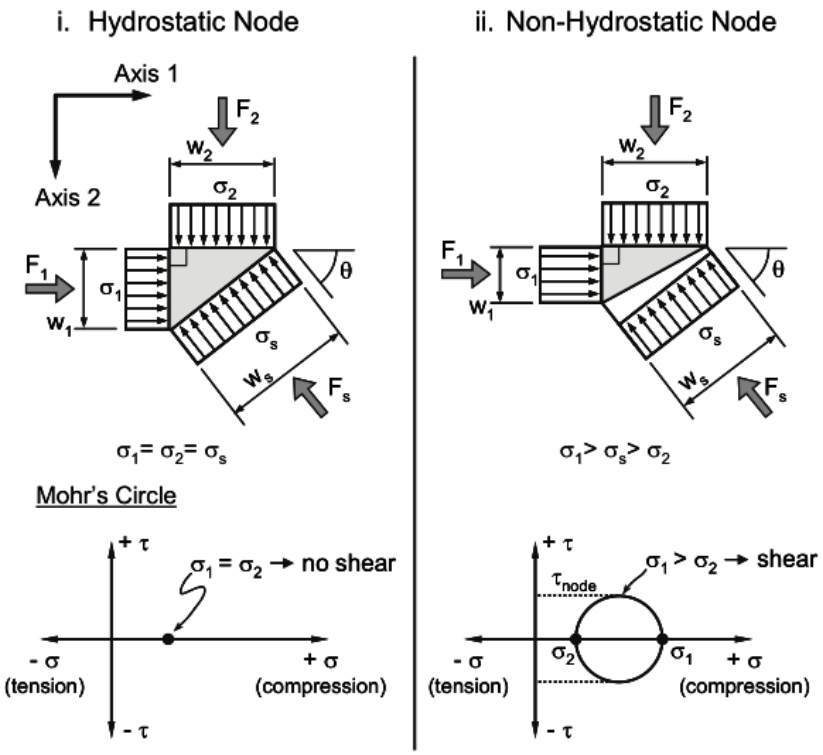

Figure 10: The difference between a hydrostatic and a non-hydrostatic node. (ACI Comittee 318, 2002)

As stated above hydrostatic nodes are impractical and impossible to realize, this refers to the impracticality to place steel reinforcement and the unrealistic geometries of the nodes (Williams et al., 2012). This is shown in figure 11.

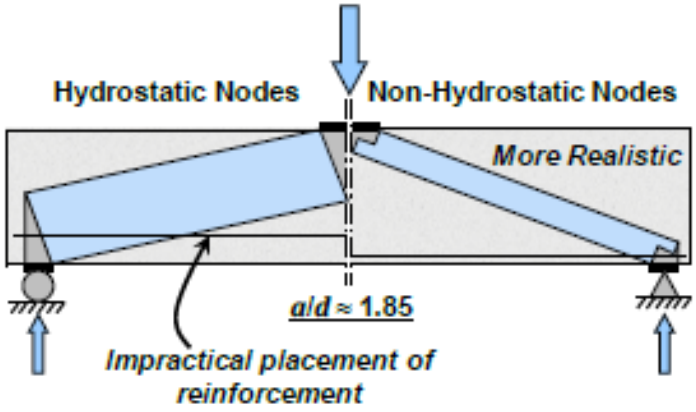

Figure 11: Impracticality of a hydrostatic node (Williams et al., 2012)

2.4 Design according to ACI

Nowadays there are many code provisions that offer guidance in using STM to design and analyze D-regions. The most important European codes are the EC2 (Eurocode 2, 2005) and fib (The International Federation for Structural Concrete, 2013), the most important American codes that describe STM are ACI 318 (ACI Comittee 318, 2014) and AASHTO LRFD (American Association of State Highway and Transportation Officials, 2017). The “Strut-and-Tie Model Design Examples for Bridges: Final Report” (Williams et al., 2012) provides a design flowchart where users of STM can base their design on. We used this flowchart together with the ACI 318-14 to explain the main steps in STM design. These provisions are explained because most papers that we used in this study often refer to or even adapt formulations from this code. STM design specifications have first been adopted into this code in 2002 in the Appendix A for the design of members that has not been explained in the core text. Since then, STM has been given a proper chapter.

For us it was important to first get to know this procedure before jumping into our critical analysis of the most current recommendations that are made in the papers that we discussed. By knowing the design STM design procedure, we could better understand the different steps and consequently we were able to locate the problems that are discussed in the papers to the right place of the procedure.

2.4.1 Design flowchart

Different authors propose some flowcharts to visualize the different steps in STM designing. A flowchart that is often used and represents well all the steps is given by Brown et al. (2006).

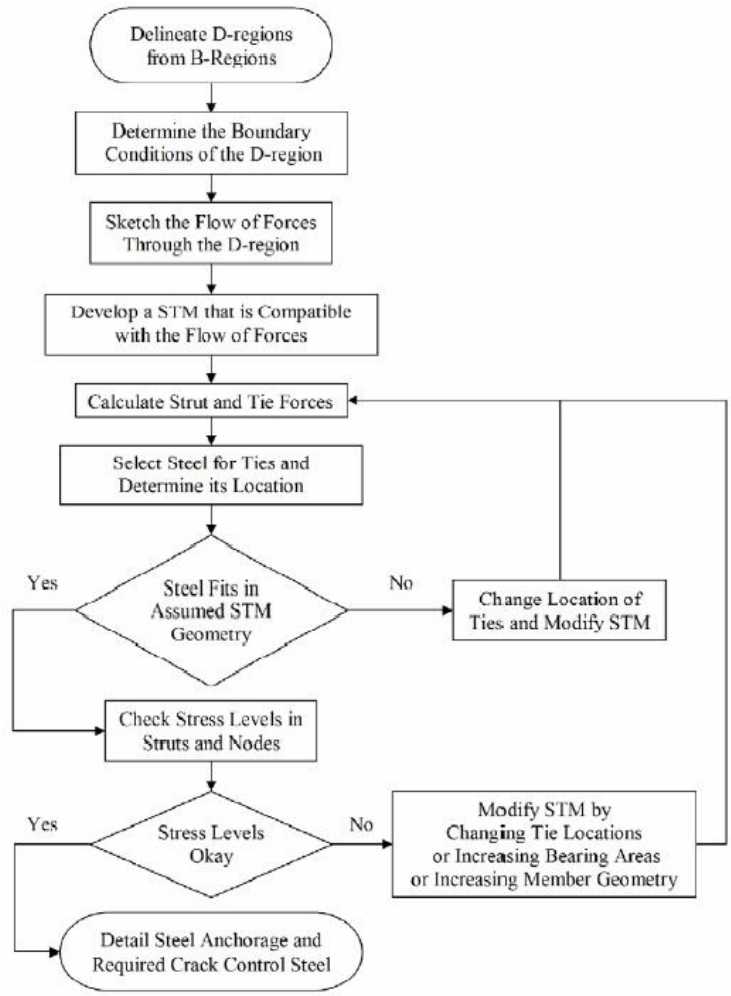

Figure 3-4: Flowchart illustrating STM steps. (Brown et al. 2006)

Figure 12: Design flowchart by Brown et al. (2006)

We can summarize this modeling procedure into a smaller amount of steps which are described below.

Step 1: Analyze the structure and the loads

Concrete structural members can be divided into B- and D-regions. The B-regions (Bernoulli regions) are the sections in the concrete member where the beam theory is valid. Assumptions are made that plane sections remain plain after loading (Euler-Bernoulli) and this is valid for those regions. The stresses within a cross-section of the concrete are linear. D-regions however don't show this linear distribution of stresses. It is for these regions that STM is used. To determine B- from D-regions St. Venants principle is used. Discontinuity regions occur on those places where there is a change of loads or a change in the geometry of the structure. St. Venants principle explains that the stress due to axial loading and bending becomes a linear distribution again on a small distance away from the discontinuity. The value that is proposed

is the depth of the cross-sectional member h, away from both sides of the discontinuity as is illustrated in figure 13.

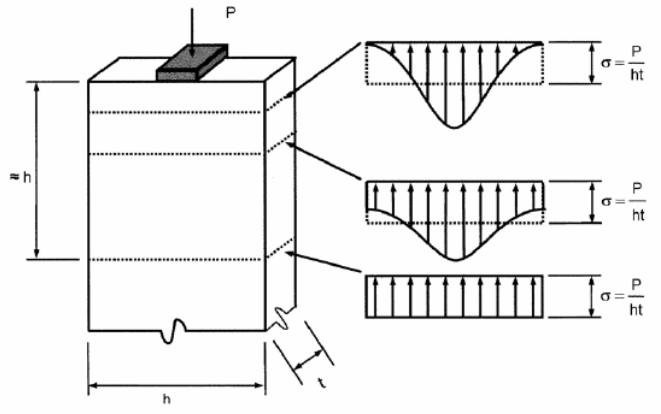

Figure 3-1: St. Venant's principle (Brown et al. 2006).

Figure 13: St. Venant's principle (Brown et al. 2006)

When applying these principles to the concrete structure, it can be divided into the both zones as in figure 14. When these zones are determined, the boundary conditions should be derived. This means all acting forces on the surface between the B/D-region. This can be done easily by using the sectional approach and to transfer these internal forces as new loads at the ends of the D-regions.

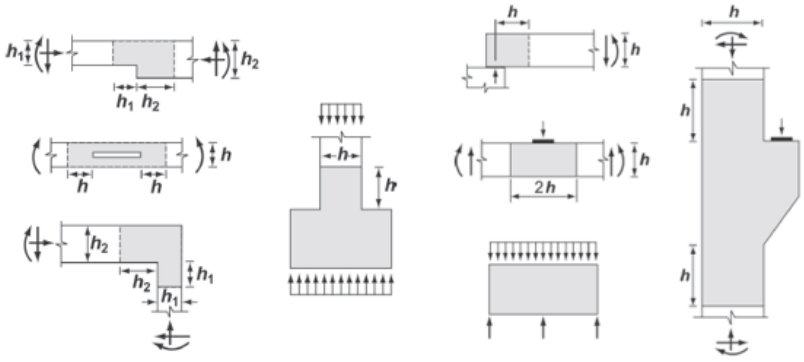

Figure 14: B/D-regions (ACI Comittee 318, 2014)

Step 2: Develop a STM

There is not a single model that can be developed for any structural member. The only thing that has to be reassured is the lower bound theorem. Loads are transferred through the structure to the supporting points by stress in the concrete and the reinforcement. As long as

the external forces don't cause exceeding of the maximal stress, then failure will not occur. For two-dimensional members like deep beams, already a lot of experiments have been done and there exist many different models. But the main idea is that struts must represent the compressive load paths as close as possible and ties must be placed where the tensile stresses are located. These stress paths are traditionally found by the use of elastic stress trajectories.

For more three-dimensional members, like pile caps, this becomes more of a difficulty. The visualization of the stress trajectories in these highly disturbed, non-linear D-regions are almost impossible to attain. Another possibility that has been developed is topology optimization techniques. The main idea of this technique is detecting finite elements within the mass of concrete that are 'active', which means that are applied with stresses. The inactive elements are deleted and consequently a solution for the geometry is derived. This method has some shortcomings as well for practitioners because FE modeling is needed. For these reasons researchers are still developing and refining STM models with their own interpretations and ideas.

Little guidance is given on the construction of a STM model in ACI 318-14. A list of some recommendations are listed below:

- The minimum angle between elements is 25°
- Follow the known cracking pattern of the structure being designed if such information is available (MacGregor & Wight, 2005)
- The path that the loads choose is dependent on the length of the path and the deformations that occur. The loads will choose the shortest path and the path with the fewest deformations (MacGregor & Wight, 2005)
- Struts cannot overlap, but ties can cross struts
- Use of a statically determinate model is recommended (MacGregor & Wight, 2005)

Step 3: calculate member forces

When a statically determinate model is used, the forces in the members can be easily calculated regarding the geometry of the model and the external forces that are applied.

Step 4: determine reinforcement in ties and check stress limits

The required amount of reinforcement for the ties can be computed by dividing the force in the tie by the product of the yield stress of the steel. The rebars must then be placed in a way that the centroid of the reinforcement coincides with the location of the tie in the STM. If the geometry of the member doesn't allow this position, then a new location should be chosen which results in a modified STM model and consequently member forces need to be recalculated.

ACI 318-14 provides the following equation to determine the strength of the ties, from which the amount of reinforcement can be calculated:

$$F_{nt} = A_{ts} f_y + A_{tp}(f_{se} + \Delta f_p)$$

Where A_{tp} is zero for non-prestressed members.

When using bottle-shaped struts, there must be a minimum amount of web reinforcement crossing the struts to prevent them from splitting due to transverse tensile stresses. The amount is given by:

$$\sum \frac{A_{si}}{b_s s_i} \sin \alpha_i \geq 0.003$$

Where A_{si} is the required reinforcement, b_s the width of the strut, s_i the spacing of this additional reinforcement and α_i the angel of the corresponding strut, see figure 15.

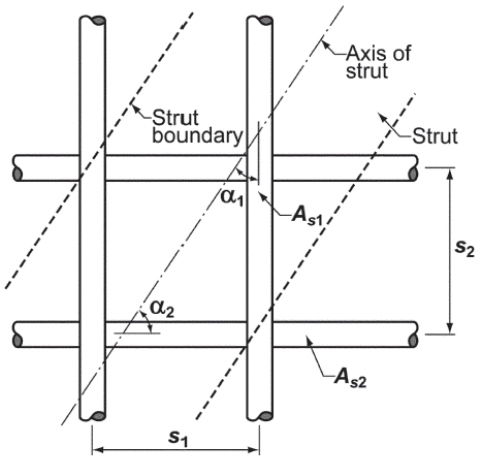

Fig. R23.5.3—Reinforcement crossing a strut.

Figure 15: Reinforcement crossing a strut

The strength of the struts is given by the following equation in ACI 318-14 chapter 23:

$$F_{ns} = f_{ce} A_{cs}$$

$$f_{ce} = 0.85\beta_s f_c'$$

In this formulation the area A_{cs} for two-dimensional models like deep beams, is calculated by the projection of the bearing area perpendicular to the axis of the strut. We can already remark here that the given formulation is hard to deal with in three-dimensional members.

The efficiency factor β_s depends on the shape of the strut and is given by the following provisions in ACI:

Table 23.4.3—Strut coefficient β_s

Strut geometry and location	Reinforcement crossing a strut	β_s	
Struts with uniform cross-sectional area along length	NA	1.0	(a)
Struts located in a region of a member where the width of the compressed concrete at midlength of the strut can spread laterally (bottle-shaped struts)	Satisfying 23.5	0.75	(b)
	Not Satisfying 23.5	0.60λ	(c)
Struts located in tension members or the tension zones of members	NA	0.40	(d)
All other cases	NA	0.60λ	(e)

Figure 16: Strut efficiency factor

The strength of nodal zones is similarly assessed by the code provision with similar equations:

$$F_{nn} = f_{ce} A_{nz}$$

$$f_{ce} = 0.85\beta_n f_c'$$

The area A_{nz} which represents the considered area of the nodal zone, is given by the area perpendicular on the axis of the strut that enters the nodal zone. Again we can make the remark that no special specifications are given for three-dimensional nodal zones accept that it should be at least the size of which is explained for two-dimensional nodal zones.

The efficiency factor β_n for calculation of the effective concrete strength of the node is given in the following table from ACI (figure 17).

Table 23.9.2—Nodal zone coefficient β_n

Configuration of nodal zone	β_n	
Nodal zone bounded by struts, bearing areas, or both	1.0	(a)
Nodal zone anchoring one tie	0.80	(b)
Nodal zone anchoring two or more ties	0.60	(c)

Figure 17: Nodal zone efficiency factor

Step 5: provide anchorage for the ties

ACI 318-14 states that the tie reinforcement shall be anchored by mechanical devices, post-tensioning anchorage devices, standard hooks or straight bar development. Because of geometrical limitations, the most used method is with standard hooks. The reinforcement should be anchored before it exits the extended nodal zone as shown in figure 18.

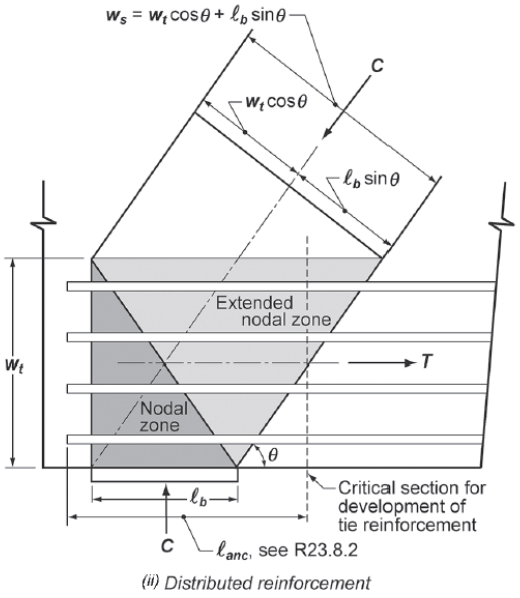

***Fig. R23.2.6b**—Extended nodal zone showing the effect of the distribution of the force.*

Figure 18: Anchorage of the reinforcement

When using standard hooks, the development length that is necessary for anchorage of the tension ties is given by the minimum of the following values from section 25.4.3 (ACI 318-14):

a) $\left(\frac{f_y \psi_e \psi_c \psi_r}{50\lambda\sqrt{f'_c}}\right) d_b$

b) $8d_b$

c) $6in.$

Where d_b is the bar diameter, f_y the yield stress of the reinforcement, λ a factor to account for light or normal weight concrete and ψ are modifications factors which can be found in Table 25.4.3.2 (ACI 318-14).

3 Improvements on Deep Beams

Deep beams are a very important structural members because they carry heavy loads over a short span from the upper structure to the substructure, for example transfer girders used in tall buildings and bridges. Although the high importance of this structural member, current design codes do not provide accurate and reliable specifications for the design and analysis of the shear capacity of deep beams. A first method that was used was providing enough depth to account for the shear strength of the deep beam and simultaneous providing enough longitudinal reinforcement based on simple beam theory to provide flexural capacity. However, deep beams are disturbed regions (D-regions) and consequently this beam theory where plane sections are assumed to remain plain cannot be used.

The second method to design deep beams is using the strut-and-tie method which captures the non-linearity of the stress distribution. Concrete compressive struts between the loads and the support points represent the compressive stress fields in the concrete, while the ties account for the reinforcing steel in the deep beam. The struts and nodes come together in the nodes. Several researchers have done experimental tests throughout the years to investigate interesting parameters of deep beams to determine the shear capacity. Based on these tests and conclusions some STM methods and improvements are proposed and tested for the effectiveness.

In this part of the Master's Thesis a table is presented as a collection of the most important and most recent improvements based on the STM to design and analyse deep beams. The main principles are explained and a critical analysis is performed for each paper.

3.1 Table of improvements

Nr.	Date	Authors	Improvements/Recommendations	Remarks
1	2014	(D. B. Birrcher, Tuchscherer, Huizinga, & Bayrak, 2014)	- The shear strength of deep beams (a/d < 2) did not increase proportionally with an increase in effective depth. - Effective depth didn't have a negative effect on the comparison between the experimental and calculated capacity of deep beams (a/d < 2) according to the strut-and-tie analysis. - Increasing depth didn't have a negative influence on the diagonal cracking load of deep beams (a/d < 2). - Once a depth of 42 in. was reached, the depth effect on the diagonal crack width was mitigated.	
2	2014	(Tuchscherer et al., 2014)	- Improved design procedure - Concrete compressive strength increasing factor when triaxial confined in nodal zones $m = \sqrt{A_2/A_1} < 2$ - Proposed maximum stresses for the faces of nodal zones	The proposed procedure gives slight modifications to the stress limits for nodal zones according to ACI318-11.
3	2014	(Garber, Gallardo, Huaco, Samaras, & Breen, 2014)	ACI 318-08 provisions for indeterminate beams are conservative.	The experimental tests that were performed were only for one specific deep beam with three random openings.

4	2016	(Shuraim & El-Sayed, 2016)	- ACI STM gives conservative predictions for HSC deep beams. - Location of upper node	The study tested the applicability of ACI STM provisions for HSC deep beams. They seemed conservative but this conclusion can't be generally adopted.
5	2016	(Liu & Mihaylov, 2016)	The two-parameter kinematic theory (2PKT) is a viable alternative to the strut-and-tie method to design and analyse D-regions.	The 2PKT method is more complex/difficult than the semi-empirical strut-and-tie model.
6	2016	(Tuchscherer, Birrcher, & Bayrak, 2016)	- The use of UT STM to reduce discrepancy between ACI 318-11/AASHTO and sectional shear design - For a/d between 2.0 and 2.5, the authors recommend limiting the ratio of the steel reinforcement to concrete capacity, V_S/V_C to 2.0. - In AASHTO changing the STM efficiency factors	
7	2016	(Su & Looi, 2016)	- Changing the nominal unreinforced strut efficiency factor β in the ACI 318-11 code to 0.7 instead of 0.6. - Proposed shear limit and shear enhancement factor: - $For\ \frac{a}{d} \leq 1, v_{c\ proposed} = v_{c\ strut} = 0.20 * f'_c$	A uncertainty factor of 0.85 needs to be taken in account for the effective unreinforced strut efficiency factor.

			- $for\ 1 < \frac{a}{d} \leq 2, v_{c\ proposed} = (v_{c\ strut} - v_{c\ code})\left(1 - \frac{a}{d}\right) + v_{c\ strut}$ - $for\ \frac{a}{d} > 2, v_c = v_{c\ code}$	
8	2016	(Mohamed, Farghaly, & Benmokrane, 2016)	They proposed a new equation to calculate the strut efficiency factor β_s in deep beams reinforced with fiber-reinforced polymer bars, using three parameters they found the most important. Those parameters are the concrete compressive strength, the shear span-depth ratio and the principal tensile strains. The equation is: $\beta_s = z * \left(f'_c\right)^a * \left(\frac{a}{d}\right)^b * (\varepsilon_1)^c$	The proposed equation is also applicable to steel reinforced deep beams.
9	2017	(Khatab, Ashour, Sheehan, & Lam, 2017)	ACI STM is recommended among existing codes for construction of continuous SCC deep beams.	The study performs an experimental investigation of specifically continuous deep beams with SCC.
10	2017	(Ismail, Guadagnini, & Pilakoutas, 2017)	All the codes should determine an effectiveness factor v' that includes the shear span-depth ratio, the concrete compressive strength, size effect and skin and vertical shear reinforcement to be able to have better shear capacity predictions.	Some codes already adept some parameters but sometimes they implement it wrong.
11	2017	(Tseng, Hwang, & Lu, 2017)	The authors proposed a new model to predict the shear strength of reinforced concrete deep beams with web openings. With a proposal for position of the nodes and formula for the horizontal reinforcement above the opening.	
12	2018	(Ismail, Guadagnini, &	New concrete effectiveness factor:	This new factor implements the effect of the

		Pilakoutas, 2018)	$\nu = \alpha \sqrt{\frac{2EG_f}{W_s\varepsilon_1}} \Big/ f_c$	effective depth, the shear span-depth ratio and the compressive concrete strength. A combination of all these factors have never been used in previous formulations.
13	2018	(Chen, Yi, & Hwang, 2018)	New cracking strut-and-tie model and proposal of a strut efficiency factor for the cracked part of the strut.	The proposed model is based on the ideologies of STM but innovates in implementing the effect of flexural cracks on the strut strength.

3.2 Analysis of papers

Using 13 papers, ranging from the year 2014-2018, an analysis was done. These papers were individually analysed and the improvements were extracted and critically discussed.

3.2.1 Depth effect in deep beams

This paper by Birrcher et al. (2014) researches the differences in the strength and serviceability of reinforced concrete deep beams due to different section depths. To do this, they calculated and experimentally tested their own specimens with an a/d of 1.2, 1.85 and 2.5 and compared them with each other.

3.2.1.1 Outline of the research

A deep beam is a disturbed region (D-region), therefore they used a strut-and-tie model to evaluate and analyse the deep beam. They used the recommendations of Tuchscherer et al. (2011) and the strut-and-tie model shown in figure 19 to predict the strength of the deep beam. The strut-and-tie model was derived using the studies by D. Birrcher et al. (2009) and Tuchscherer et al. (2011).

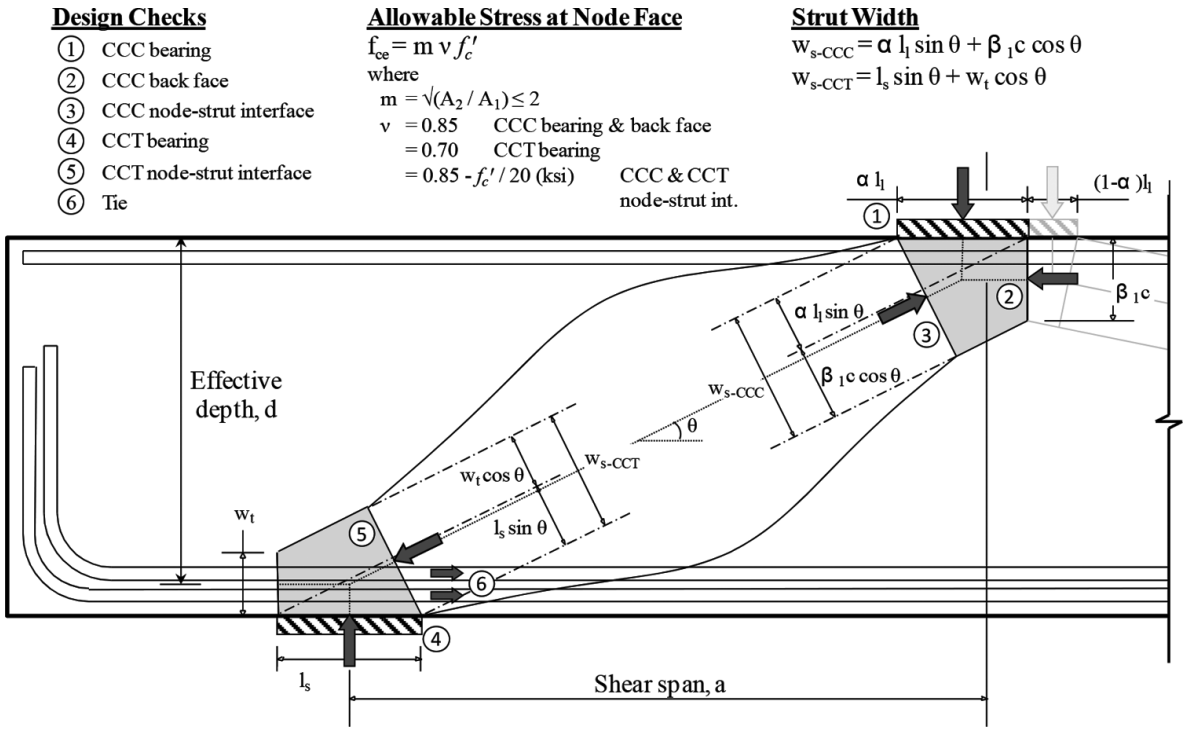

Figure 19: The used strut-and-tie model

These studies relied on a vast database of deep beam tests and the provisions found in ACI 318-08 Appendix A, AASHTO LRFD 2008, and the concrete bulletin of the International Federation of Structural Concrete (fib 1999). This new method provided a less complex, more correct method but just as conservative as the before mentioned design codes and specifications. The results of the V_{test}/V_{calc} vs effective depth can be seen in figure 20.

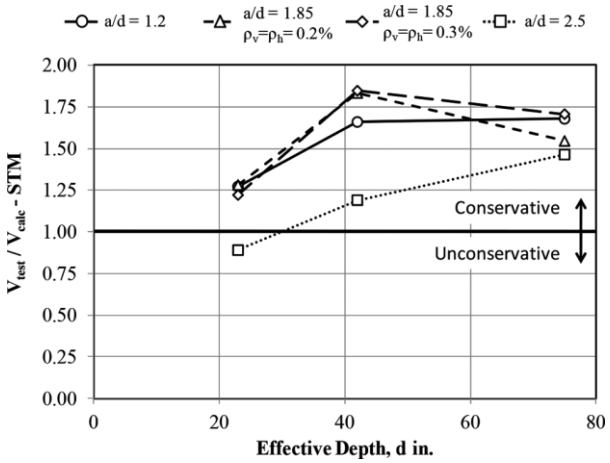

Figure 20: Experimental results of V_{test}/V_{calc} versus effective depth

The geometry of nodal zones are designed in a particular way so it represents the stress distribution as accurate as possible.

3.2.1.2 Discussion

This paper gives us some recommendations for designing deep beams with an a/d ratio lower than two, deep beams comply in general to this limit. These recommendations can be kept in mind by designers when designing deep beams. They can't be really adopted to be implemented in code provisions but are more general rules of thumb.

The first recommendation that was in the paper was that the shear strength of deep beams (a/d < 2) did not increase proportionally with an increase in effective depth, this can be seen in figure 20. Instead the strength of a deep beam is dependent on the compressive strength of the nodal zones, the compressive strength of the direct strut and the force in the primary tension tie. Because the shear strength doesn't increase proportionally to the depth, we can conclude that the sectional approach is inappropriate to analyse a deep beam. This is true, because it is widely known that the strut-and-tie analysis is far more superior to analyse D-regions in concrete members. If the sectional approach was used to determine the shear strength in deep beams, then the comparison with the effective depth would result in the conclusion that the shear strength is increasing proportionally when the effective depth increases. Using this

recommendation when designing deep beams can lead to less over dimensioned designs of deep beams resulting in less concrete use and less producing costs.

The second recommendation states that the effective depth didn't have a negative effect on the comparison between the experimental and calculated capacity of deep beams (a/d < 2) according to the strut-and-tie analysis. The results of V_{test}/V_{calc} were relatively uniform with the increasing depth, particularly for the 42 and 75 inch specimens. This could be the case because of the fact that the used strut-and-tie model accounts for the main variables that normally affect the capacity of a deep beam, especially regarding the stress conditions in nodal zones.

The third recommendations are: that the increasing depth didn't have a negative influence on the diagonal cracking load of deep beams (a/d < 2). When a/d was higher than two, there was a reduction in the diagonal cracking load. The cracking loads V_{crack} were first normalized by $\sqrt{f'_c}b_w d$. This was done to seek for relations between values. Deep beams are designed to carry heavy loads and that's why the increasing depth didn't have a negative effect. When increasing the depth, the a/d increases (higher than 2) and the deep beam becomes a slender beam therefore the depth effect had a negative impact on the diagonal cracking load.

The last recommendation was that once a depth of 42 in. was reached, the depth effect on the diagonal crack width was mitigated.

We trust the authors of this paper because after we compared the experimental strength vs the effective depth between the authors and three other models, somewhat the same trend can be seen in the graphs. Because of this, the results and recommendations can be trusted.

3.2.2 Evaluation of existing strut-and-tie methods and recommended improvements

The aim of this study by Tuchscherer et al. (2014) is on providing recommendations on the existing design procedures for deep beams and D-regions using STM. The ideas of three major codes ACI 318-11, fib and AASHTO LRFD are followed to keep the proposed improvements compatible with these existing design procedures.

3.2.2.1 Outline of the research

The first step in the design procedure is the choice of an appropriate model. To be consistent with the existing guidelines, the authors chose single strut-and-tie model with non-hydrostatic nodes as is presented more in detail in figure 21.

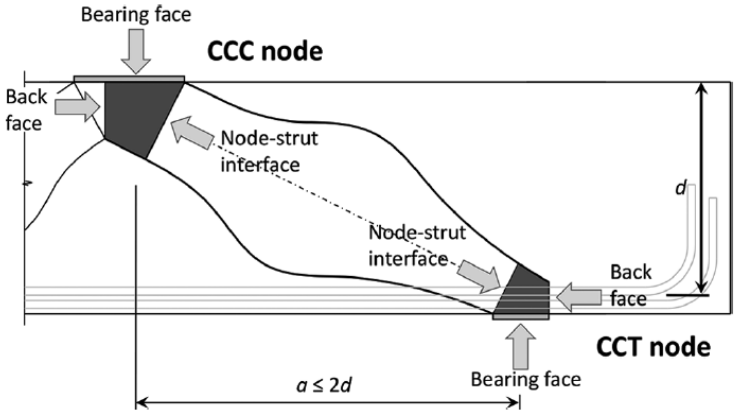

Fig. 2—Direct bottle-shaped strut bounded by CCC and CCT node at each end.

Figure 21: The single strut-and-tie model with non-hydrostatic nodes

The focus for improvements in the design procedure in this study is on the definition of the stress limits for the bearing face, back face and node-strut interface of the nodal zones.

The strength of nodal zones is given by the following equation according to ACI 318-11:

$$F_n = f_{ce} \times A_{nz}$$

where f_{ce} is the effective compressive strength of the concrete and is calculated by:

$$f_{ce} = m \times v \times f_c'$$

The authors propose to use an increasing factor of the compressive strength with a value of $m = \sqrt{A_2/A_1} \leq 2$ to account for triaxial confinement for nodal zones that are triaxially confined by enough concrete. This factor is the same is can be found in the ACI 318-11.

The effectiveness factor for the different faces of the nodal CCC and CCT zones can be summarized in the table 1 below.

Tabel 1: Proposed strut effectiveness factors

Element	**Design check**	**Allowable stress (proposed)**	**Allowable stress (ACI 318)**
CCC node	Bearing	$0.85f'_c$	$0.85f'_c$
	Back face	$0.85f'_c$	$0.85f'_c$

	Node-strut interface	0.45≤0.85-f'_c/138MPa≤0.65	0.64f'_c
CCT node	Bearing	0.7 f'_c	0.68f'_c
	Back face	Not to be checked	0.68f'_c
	Node-strut interface	0.45≤0.85-f'_c/138MPa≤0.65	0.64f'_c
Tie	Tie	f_y	f_y

The geometry of the different faces of the nodes can be seen in figure 22.

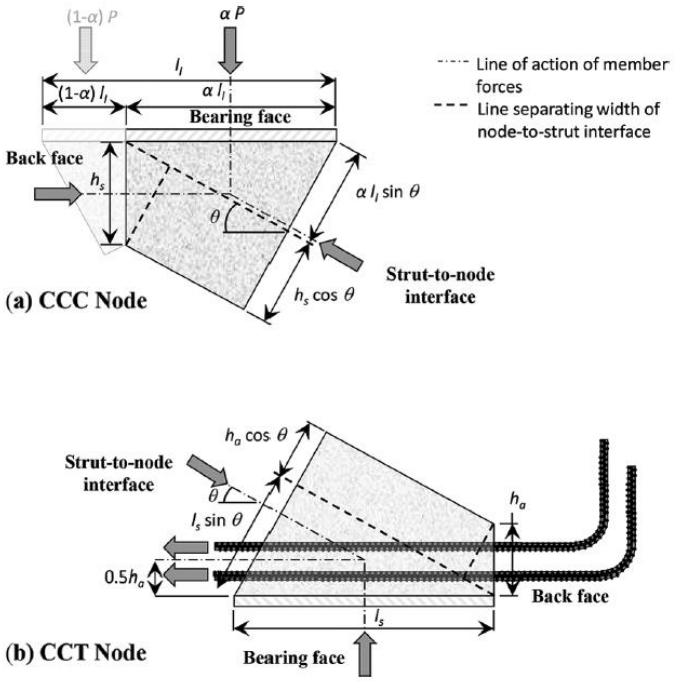

Fig. 3—Proportions for: (a) CCC; and (b) CCT nodal region.

Figure 22: The geometry of the different faces of the nodes

3.2.2.2 Discussion

The factor for enhancing the strength of the concrete when triaxially confined is copied from ACI 318-11 so this presents not a real improvement. However, it is not mentioned explicitly in ACI STM provisions that this is allowable. The idea is adopted from fib provisions and gives more accurate predictions. For this reason we conclude that this is allowable and ACI should consider this into the code.

Considering the stress limit checks, after all, there have only been two big changes suggested.

The first one is the limit of $0.7f'_c$ instead of $0.68f'_c$ for the bearing stress in the CCT node. This change is made based on a very scarce dataset of deep beams failing because of this stress limit boundary. This is only a slight change and therefore we conclude that the slightly adapted formulation cannot be implemented or replace the current provision because of this proposal.

A second improvement is the stress limit of the node-strut interface of both CCC and CCT nodes. Where the ACI currently uses a single factor of $0.68f'_c$, the proposed model introduces an efficiency factor that diminishes with an increasing compressive strength as given in table 1 above. This seems a valid idea to us because a similar formulation is used in AASHTO LRFD and it is theoretically supported. In high strength concrete the cement paste can become stronger than the aggregates that are used. Consequently above a certain level of concrete strength, the failure of aggregates is determinative and could occur faster than the failure of the concrete.

The overall objectives from the authors seem to have been reached regarding figure 23. They were able to develop an STM procedure that is simpler and more accurate than current provisions except from fib provisions. The biggest change with current ACI provisions is the new diminishing strut-to-node effective stress factors (strut efficiency factor) with increasing concrete strength. We could suggest to adopt this formulation into the code provision.

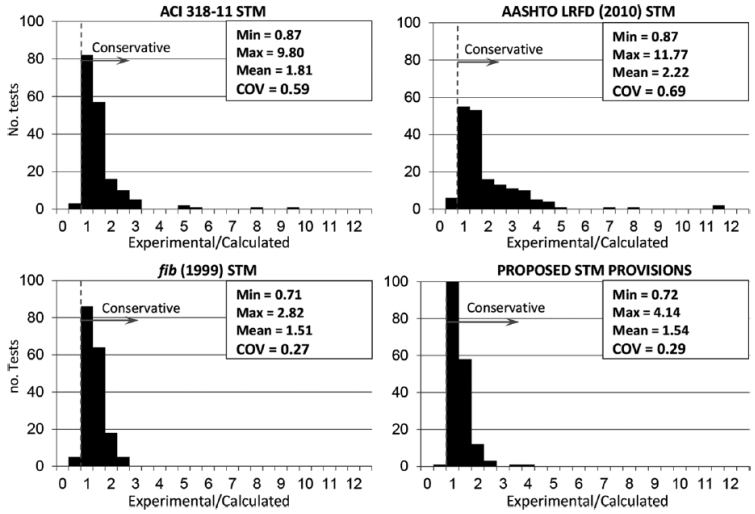

Fig. 5—Statistical comparison of ratios of experimental-to-calculated capacity for specimens in evaluation database (N = 179).

Figure 23: Comparison experimental results versus code provisions

3.2.3 Experimental evaluation of strut-and-tie model of indeterminate deep beam

This research by Garber et al. (2014) tests the conservativeness of the ACI 318-08 STM provisions on indeterminate deep beams, moreover with extreme discontinuities.

3.2.3.1 Outline of the research

Four different STM models were developed purely based on the elastic flow of stress generated by a finite-element model. In figure 24 can be seen that three of them follow more orthogonal geometries while one of the layouts follows more closely the paths of the stresses developed by the FEM.

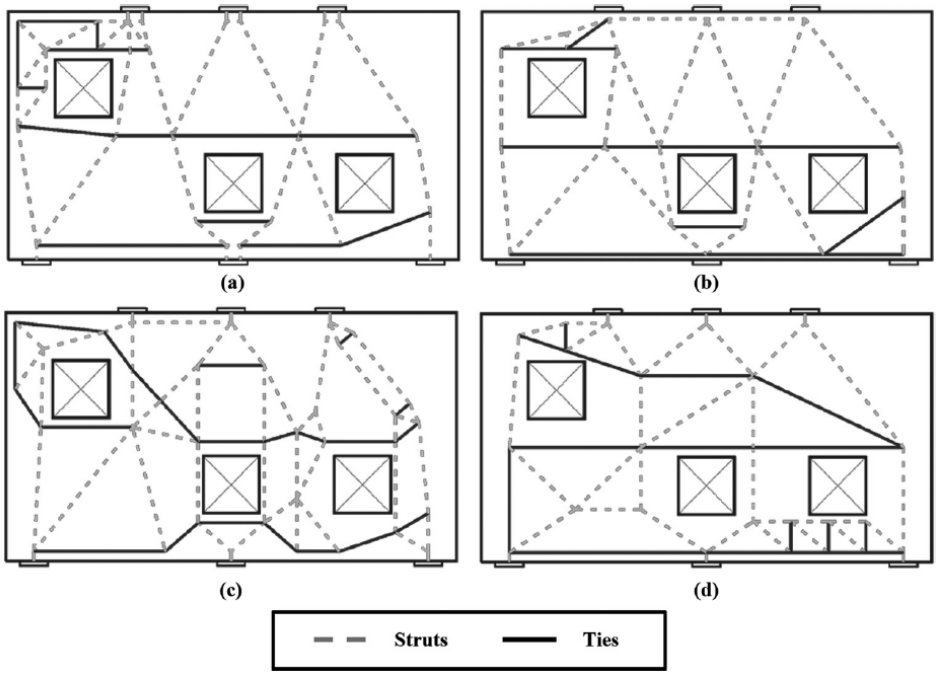

Figure 24: Flow path stresses

Observations:

- All of the specimen showed a higher capacity than the design capacity with ACI 318-08
- Reinforcement layout following the stress paths more closely gives the most economical solution
- Node capacity is increased when properly confined

3.2.3.2 Discussion

We strongly doubt the usefulness of the conclusions of this paper. The main goals that were demonstrated make perfect sense and isn't innovative. It is logical that when confining the

concrete in nodal zones with reinforcement, that the capacity will increase and that this could cause a change of load path and consequently another mode or place of failure. However, these logical theoretical findings have been proven by the authors which isn't always that evident. Confining these zones does have a positive effect on the strength.

The fact that following the stress paths more closely with the strut-and-tie model also isn't something new and just confirms the principle ideas of the strut-and-tie method.

We cannot conclude that ACI provisions are conservative for indeterminate structures only based on this study. Only four specimen with different reinforcement layout were tested as a first limitation. Secondly there could be thousands of positions for the three openings in the beam. Therefore this study isn't representative to make any conclusions about the conservativeness of ACI provisions for indeterminate deep beams.

3.2.4 Experimental verification of strut-and-tie model for HSC deep beams without shear reinforcement

This study by Shuraim & El-Sayed (2016) performs an experimental campaign of four-point bending tests on 18 high strength concrete (HSC) deep beams. The main parameters that are investigated are the effect of the shear span-depth ratio, longitudinal reinforcement and the member depth. Considering the strut-and-tie method lots of tests have been conducted to check the applicability of the method on normal strength concrete, but there is a lack of verification of the formulations for high strength concrete. Two assumptions of the model that have been checked are the position of the upper node and the safety of the strut efficiency factors that are provided in the ACI 318.

3.2.4.1 Outline of the research

The STM model that is used is not just the single strut-and-tie model which is applicable for a single concentrated load, because the tests that were performed are four-point bending tests. Therefore a model is used with a horizontal upper strut in the middle between the loads as shown in figure 25.

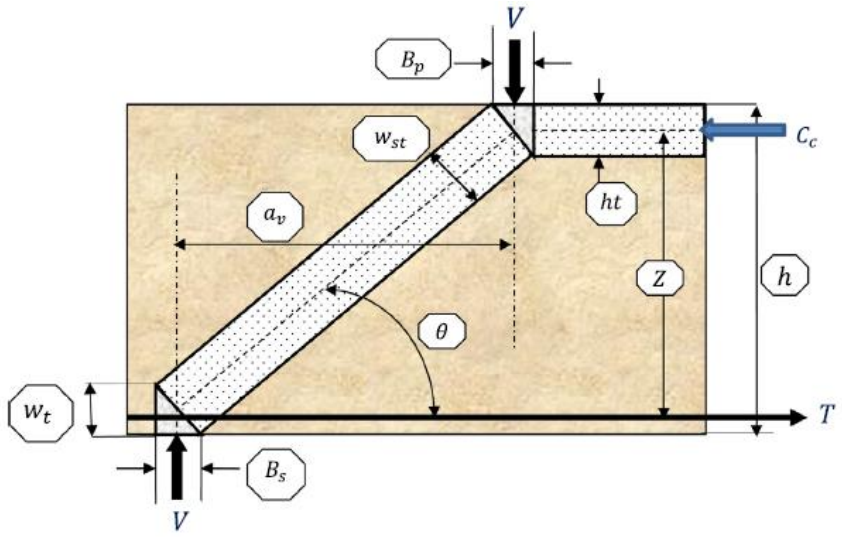

Fig. 3. Schematic representation of strut and tie model showing notations.

Figure 25: The used strut-and-tie model with an upper horizontal strut between point loads

The height of the upper node in this study is given in two ways. The depth of the horizontal strut is first taken as the depth of the flexural compression depth *c* which can be easily determined from equilibrium as demonstrated in the paper. The second assumption is c_{max} which is attained when the steel stress reaches the yield stress. Calculation of c and c_{max} can be seen in figure 26.

$$c = \frac{V\,a_v}{0.85\,f_c'\,b\left(d-\frac{\beta_1 c}{2}\right)} \leq \frac{A_s\,f_y}{0.85\beta_1 f_c'\,b} = c_{max}$$

Figure 26: Calculation of flexural compression depth

Observations:

- Using c_{max} gives the best STM predictions for the ultimate capacity
- Concrete effectiveness factors for the struts are shown to be conservative
- Concrete effectiveness factors are not able to capture size effect

3.2.4.2 Discussion

It seems logical to us that c_{max} gives the best predictions of the ultimate strength in the tests were enough reinforcement is provided to prevent flexural failure. By enhancing the width of the strut, the area of the nodal zone increases which increases again the width of the strut and consequently the strength of the strut. Nevertheless, these logical assumptions need to be tested and proven, which is not always evident.

However it seems a little too fast to conclude that this configuration of the model can be seen as the best in general. The limitations of this research are the low amount of tests performed and the specific test setup of the four-point bending test. This assumption should be tested against a bigger dataset of deep beams which are also tested with a single concentrated load.

The strength predictions don't remain on an equal level of accuracy when varying the depth of the beams. This clearly indicates that the effect of the depth isn't captured by the current and simple concrete effectiveness factors provided by the ACI. This is an important finding which has been confirmed by El-Sayed & Shuraim (2015) and Mihaylov et al. (2013). Therefore concluding and being satisfied with the conservative predictions of the small set of HSC deep beams tested in this study can't be approved. Further development on effectiveness factors, especially for HSC in this case, is needed.

Considering the use of STM for designing HSC deep beams based only on this study, some remark can be made. On the one hand it has been proven for the given database that ACI effectiveness factors for struts and nodal zones was observed to be conservative. On the other hand this factor was not able to capture the effect of the investigated parameters which were reinforcement ratio, shear span-depth ratio and depth. As already explained in a previous discussed paper by Tuchscherer et al. (2014), high strength concrete behaves different from normal strength concrete and it was shown that a diminishing strut efficiency factor with increasing concrete strength could be better used.

3.2.5 A comparative study of models for shear strength of reinforced concrete deep beams

This papers by Liu & Mihaylov (2016) compares 10 of the more recent models on the evaluation of the shear strength of reinforced concrete deep beams by using a database of 574 deep beam tests with an $a/d < 3$. In this comparison the semi-empirical strut-and-tie model by Russo et al. (2006) and the two-parameter kinematic theory (2PKT) by Mihaylov et al. (2013) were found to be the most accurate with the least scattered predictions. The strut-and-tie model has an average value for V_{exp}/V_{pred} of 1.00 and a coefficient of variation of 19.8% while the 2PKT method has an average of 1.08 and a COV of 15.4%. These two methods were then further analysed.

3.2.5.1 *Outline of the research*

First the semi-empirical strut-and-tie model by Russo et al. (2006) is briefly explained. Semi-empirical means that the theoretical model also contains factors that are obtained by experimental testing of deep beams.

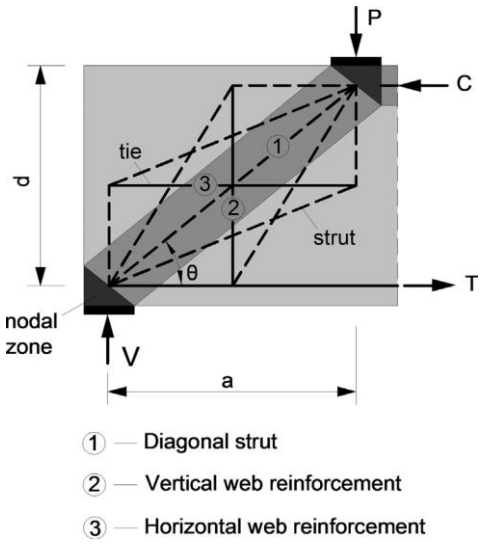

Figure 27: The semi-empirical strut-and-tie model

In figure 27 you can see the general design of the strut-and-tie model used in this paper. There are three mechanisms, first you have the direct diagonal strut between the two nodal zones, second and third you have a truss mechanism for the vertical and horizontal web reinforcement.

The two-parameter kinematic theory (2PKT) is built on the kinematic description of the deformation patters in deep beams. Therefore this model can predict shear strength and deformation patters near failure. When there is a critical diagonal crack, that divides the shear span into two parts, then there is a possibility of shear failure along the crack (figure 28).

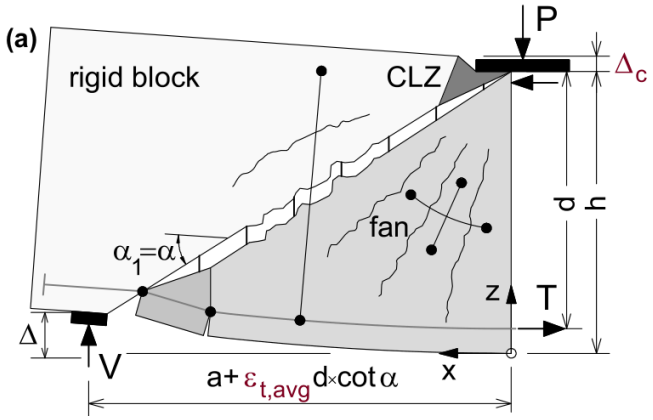

Figure 28: Shear failure along the crack (2PKT)

The lower part of the crack is then modelled as a fan of rigid radial struts and the upper part is modelled as a rigid block.

Both of these models predicted that the shear strength decreases when increasing the a/d value and also that the degree of decrease of shear strength can be reduced or even eliminated by using transverse reinforcement. But while the semi-empirical strut-and-tie model predicted an overestimate of the capacity of the specimens, the 2PKT method predicted more the average experimental values.

Regarding the transverse reinforcement in a deep beam, both models predicted that the shear strength would increase when adding more transverse reinforcement and that the rate of increase depends on the a/d ratio, the bigger the a/d, the faster the shear strength increases. The difference between the two models is that the strut-and-tie method has a linear relationship between the shear strength and the transverse reinforcement while the 2PKT method suggests that the effect of transverse reinforcement on the shear strength is eliminated when the value is more than 0,7%.

Regarding the longitudinal reinforcement in a deep beam, the strut-and-tie method concludes that when larger amounts of longitudinal reinforcement is used the diagonal struts are larger and stronger. While the 2PKT method also gives a good prediction of the longitudinal reinforcement, it underestimates the shear capacity when there are large reinforcement ratios and small yield strengths.

The strut-and-tie model doesn’t account the size effect for shear in deep beams. While the 2PKT method does account for the size effect, the decrease in shear because of the size is well captured by this method.

3.2.5.2 Discussion

In this study ten models to analyse and design deep beams were compared. From these ten models the best two were taken and further analysed using a data base of a little less than 600 deep beam tests. These were the semi-empirical strut-and-tie model of Russo et al. (2006) and the two-parameter kinematic theory of Mihaylov et al. (2013). They theoretically calculated the chosen deep beams and compared it to the experimentally obtained values of the database. From this comparison some conclusions could be made. The STM had an average of 1.00 and a coefficient of variation of 19.8% while the 2PKT method had an average of 1.08 and a coefficient of variation of 15.4%, both models were rather good and accurate.

Our opinion is that while strut-and-tie method is widely used to evaluate and analyse deep beams, and more in general D-regions, the model still doesn't account for every parameter, for example the size effect in shear. Knowing this and the fact that the 2PKT method does account for the parameter of size effect in shear, this method could be a viable and useful option to evaluate and analyse deep beams or use it as a complementary option next to the strut-and-tie method. However both models designed the deep beams rather well, neither of the two were perfect. We personally, and in general everybody, would choose to use the strut-and-tie model because in our opinion it's more simple and graphical to use than the 2PKT method which is more difficult to implement.

Further on, this comparative study was only focused on deep beams so you can't automatically assume that it will also be a viable and useful tool to evaluate and analyse other concrete members with D-regions such as pile caps, corbels, dapped-end beams, etc. To implement this 2PKT method for other D-regions, the model should to be compared an tested on other elements with D-regions. Using this comparison, changes can be made to the model so that it is general applicable.

Implementation of the 2PKT model into a code provision is rather difficult because nowadays every code provision has the strut-and-tie method implemented in it and keeps improving this model.

3.2.6 Reducing discrepancy between deep beam and sectional shear-strength predictions

A lot of codes, as the ACI 318-11 and AASHTO LRFD (2010), specifies that when $a/d < 2$ you should use strut-and-tie model and when $a/d > 2$ the sectional approach should be used for shear strength predictions. This is not correct because the transition between these two methods is gradual, though the codes need to set some kind of limit differentiating them. With this paper (Tuchscherer et al., 2016), the authors wanted to reduce the discrepancy between strut-and-tie modelling and sectional shear strength prediction when the shear-span to depth ratio is around 2. To accomplish their goal of identifying the causes of this discrepancy and recommend improvements, they assembled and analysed 905 shear tests on deep beams.

3.2.6.1 Outline of the research

The problem faced in this paper is that when using the code provisions of ACI 318-11 and AASHTO LRFD (2010) to compare the capacity of a deep beam with an a/d of 1.99 and 2.01,

there is a huge difference regarding the capacity of the deep beams. This is the discrepancy that is mentioned above and can be seen in figure 29.

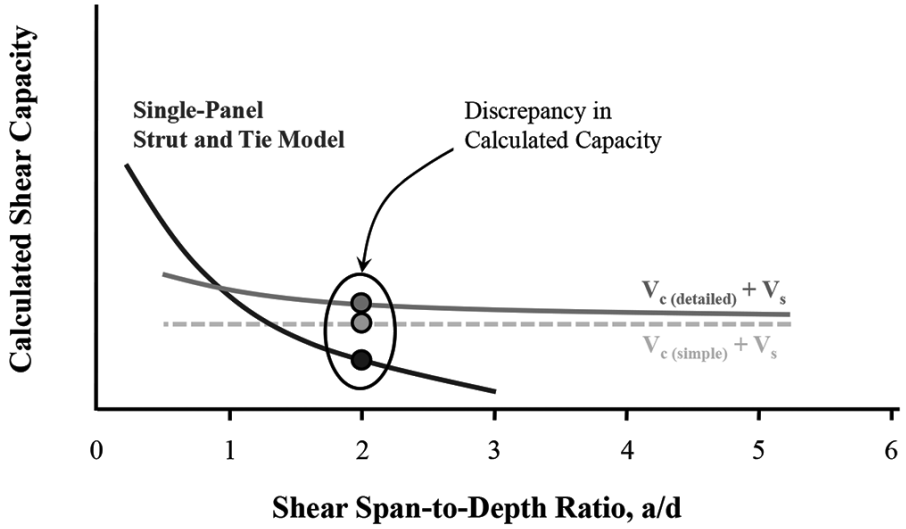

Figure 29: The discrepancy at an a/d ratio of 2

The strut-and-tie model that is used, is a single-panel truss model with non-hydrostatic nodal zones so that it can represent all of the deep beam shear tests in the database. Figure 30 and figure 31 gives a better understanding of the used model.

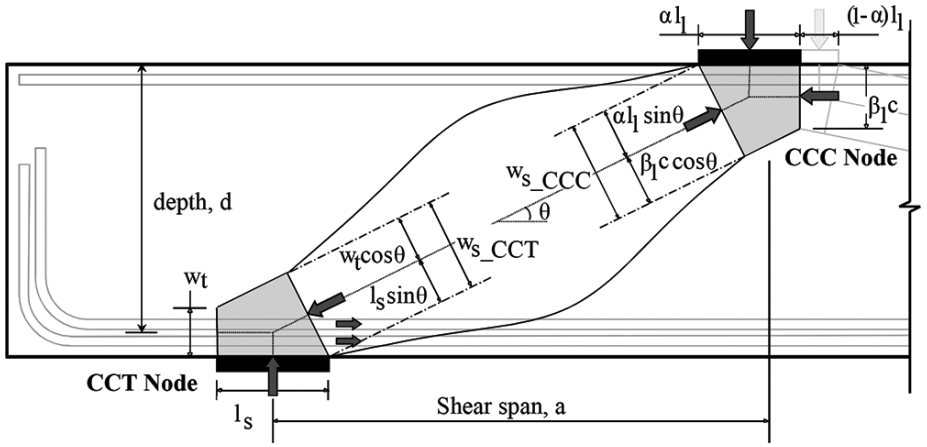

Figure 30: The used strut-and-tie model

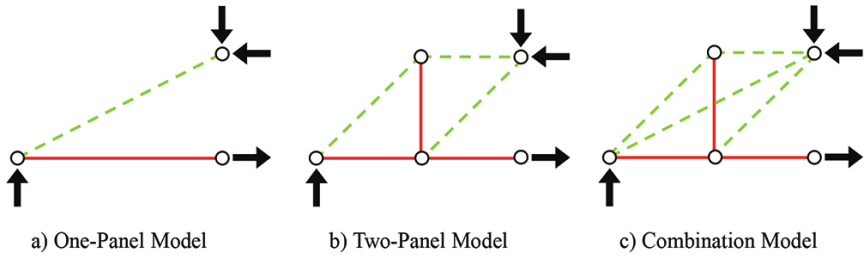

Figure 31: Different kind of panel models to be used in STM

The strains were calculated beforehand so they could compare it with the actual, measured strains the deep beam. There were two values, namely ε_{1_STM} and ε_{BEAM}. ε_{1_STM} represents the calculated strain in the tie of the single-panel STM model and is constant and ε_{BEAM} represents the strain in the reinforcement of a Bernoulli beam. The strains were more or less the same around the load points but around the shear span there was a reduction. This reduction could be caused by the fact that a part of the applied load was transferred via a multi-panel or sectional shear model to the support.

With an a/d of 1.85 the measured strained is closer to ε_{1_STM} and the difference between the measured strain and ε_{1_STM} was exactly one third of the difference between ε_{1_STM} and ε_{BEAM}. This implies that one third of the applied load is transferred via a sectional shear model to the support and two third via single-panel STM. On the other hand you have deep beams with an a/d of 2.5, in this case it's the other way around. Here the measured strain is closer to ε_{BEAM} and the difference between the measured strain and ε_{1_STM} was exactly two third of the difference between ε_{1_STM} and ε_{BEAM}. This implies that two third of the applied load is transferred via a sectional shear model to the support and one third via single-panel STM. When the a/d is 1.2 the measured strain is almost identical to ε_{1_STM}. The applied load is exclusively transported to the support through a single-panel STM. Because of these results we can conclude that the transition between the single-panel STM and sectional shear model is gradual.

Elements with an a/d value between 1.85 and 2.5 transfer their applied loads around 30-60% via two-panel model. Because of this the authors considered two other cases. First a case with 75% load via one-panel and 25% via two-panel. Second a case where the applied load was evenly split between one- and two-panel STM. With the second case the authors observed a small improvement in the accuracy of the prediction of the shear strength.

3.2.6.2 Discussion

The authors evaluated the ACI 318-11 and AASHTO LRFD (2010) sectional shear provisions. Because they check the sectional shear provisions, the a/d ratio is ranging from 2.0 to 2.5. They divided the experimental shear strength by the estimated strength calculated using the aforementioned sectional shear design and plotted the results versus the ratio of steel reinforcement to concrete capacity (V_S/V_C). The data can be find in figure 32 and they could come to the conclusion that it's rather conservative. We agree with the authors that the discrepancy between STM and sectional shear design should be addressed. Because of the high level of conservation, it is shown that the sectional design is not appropriate to analyse and design deep beams. Nowadays this is already widely known in the field of deep beams.

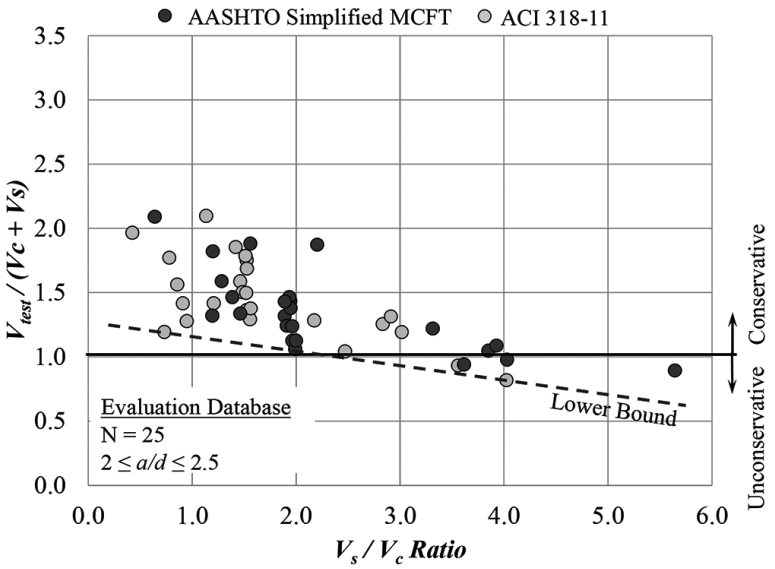

Figure 32: Level of conservatism in sectional shear provisions

As mentioned in the paper, the transition between the single-panel STM and sectional shear model is gradual. This is logical because concrete behaviour never changes from one instant to another instant, everything goes gradually to another state. However it's understandable that there need to be some kind of distinction between using STM or sectional design in code provisions.

The authors recommend to limit the ratio of steel reinforcement to concrete capacity (V_S/V_C) to 2.0 for concrete deep beams with an a/d between 2.0 and 2.5. As you can see on figure 32, we totally agree with the authors about limiting the V_S/V_C ratio and we trust in their judgement. After consulting with the ACI 318-11 and AASHTO LFRD (2010) code we can say that they still haven't changed or added this to their provisions, however it is easily implementable into the code provisions.

An improvement in AASHTO is changing the STM efficiency factors. In AASHTO they likely use the STM efficiency factor calculated for hydrostatic nodes also on non-hydrostatic nodes. Because of this the predictions of strength are overly conservative and therefore not economical to perform. We think it's not right to use STM efficiency factors calculated for hydrostatic nodes to be used for non-hydrostatic nodes because the conditions these nodes are in, are not the same. Hydrostatic nodes are described as quite balanced nodes, where all compressed faces are similar, having the same area around the node.

The authors also stated that with the use of UT STM the discrepancy is greatly reduced. The UT STM is a proposed model by Tuchscherer et al. (2014). Compared to the AASHTO LFRD (2010), the discrepancy is reduced by 75% (figure 33) and compared to the ACI 318-11, it was

reduced by 50% (figure 34). It is noted that the UT STM is not derived to reduce the discrepancy between STM and sectional shear design. The good results obtained by the UT STM is caused by performing a calibration of the process with data from the evaluation database, the experimental program and from existing STM specifications. Using these conclusions, the UT STM could be a good tool to analyse and design deep beams that have an a/d ratio between 2.00 and 2.50.

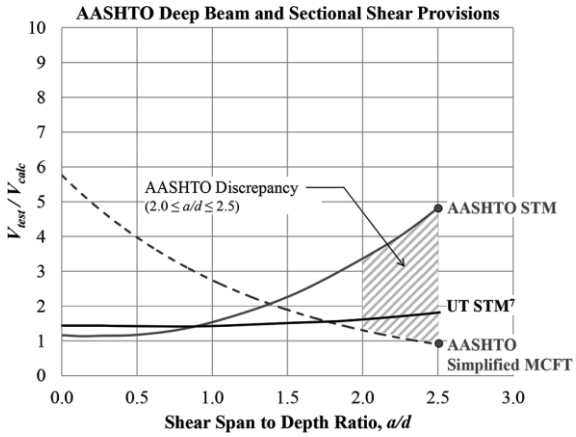

Figure 33: Level of conservatism of AASHTO

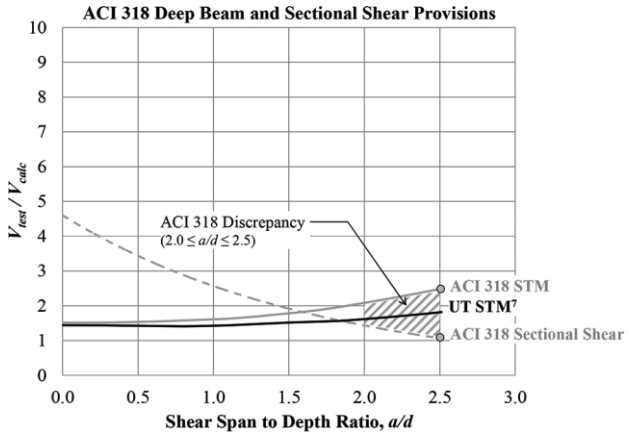

Figure 34: Level of conservatism of ACI

3.2.7 Revisiting unreinforced strut efficiency factor

In this paper by Su & Looi (2016), the compressive strength of struts in deep beam without stirrups is investigated using different strut angles and concrete strength. In doing so, the discrepancies of the strut efficiency factor between different codes were studied and the authors presented some proposals. A single constant for the unreinforced strut efficiency factor was introduced by the authors, this is also the case in the ACI 318-11. The difference between the authors proposition and the ACI 318-11 code is that the proposed constant is less conservative.

3.2.7.1 Outline of the research

As said above there were two parameters that varied regularly in this research, these two were the primary strut angle and the concrete strength. Designing the deep beams that were tested, the authors used the ACI 318-11 section A. The shear-span to depth ratio of the designed beams were 1.73, 1.00 and 0.58 respectively. The used strut-and-tie model is displayed in figure 35.

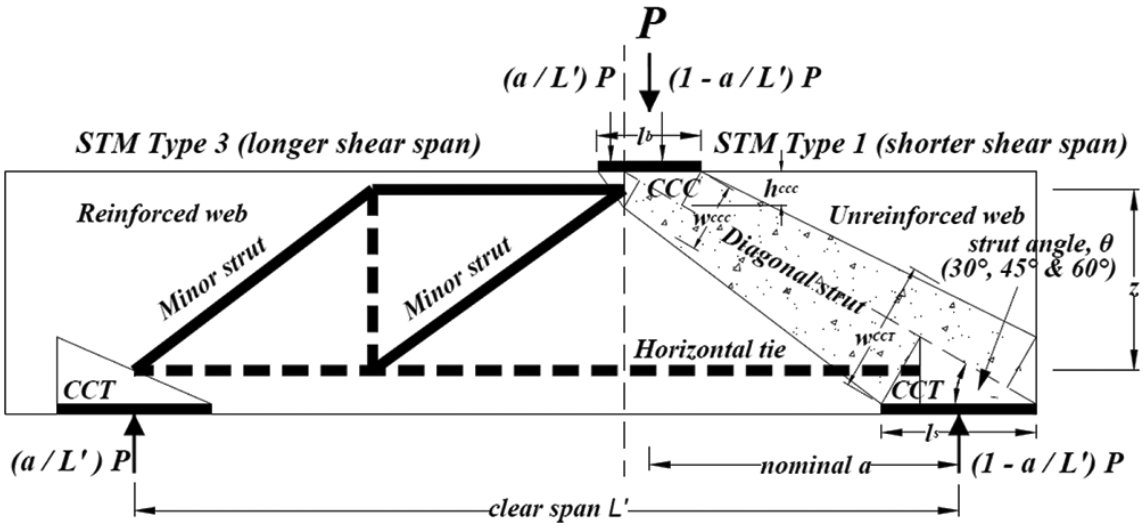

Figure 35: The used strut-and-tie model

The unreinforced strut efficiency factor of the test specimens with different concrete strength and different strut angles was calculated using following equation:

$$\beta = \frac{f_{strut}}{f'_c} = \frac{\frac{1-a}{L'} * P}{\sin(\theta) * b * w * f'_c}$$

- f_{strut} : strength of the strut
- f'_c : strength of concrete
- $\frac{1-a}{L'} * P$: describes the peak loads on the deep beam
- $\sin(\theta)$: describes the strut angle
- $b * w$: these are the width and extent of cracks

This equation is defined as a fraction of the uniaxial strength.

The results of the experimental testing were then compared to three major codes, namely the ACI 318-11, EC2 and CSA. Also the results were compared to seven other models. In the end the ACI 318-11 had the closest average value to 1.00 and the lowest coefficient of variation (COV) of 0.18. Therefore their conclusion was that the ACI 318-11 code, with a constant value

for the unreinforced strut efficiency factor, fits reasonably good with the experimental tests and was sufficiently conservative. This study found an average of 0.8 for the unreinforced strut efficiency factor β.

Following this outcome of the study, the authors proposed to elevate the nominal unreinforced strut efficiency factor from 0.6 to 0.7, this can be seen in figure 36. The uncertainty factor of 0.85, that accounts for the stress-strain field and truss model, was left unchanged. This uncertainty factor isn't explicitly mentioned in the ACI 318-11 code, but can be found in the equation to calculate the effective compressive strength of concrete in a strut f_{ce}.

$$f_{ce} = 0.85 * \beta_s * f'_c$$

Using $0.85 * \beta_s$ the effective unreinforced strut efficiency factor can be calculated, resulting in a value of 0.6 when using the aforementioned 0.7 as nominal unreinforced strut efficiency factor β_s.

In the ACI 318-11 code the conventional shear stress limit for sectional design is dependent on the square root of the concrete strength. Statistical analysis of the shear stress for group 2 specimens (a/d < 1.0) showed that the shear stress was in strong correlation with the concrete strength. Regarding their test results, they presented a lower-bound shear limit corresponding to the strut efficiency limit of 0.20*f'$_c$. This limit is shown in figure 36.

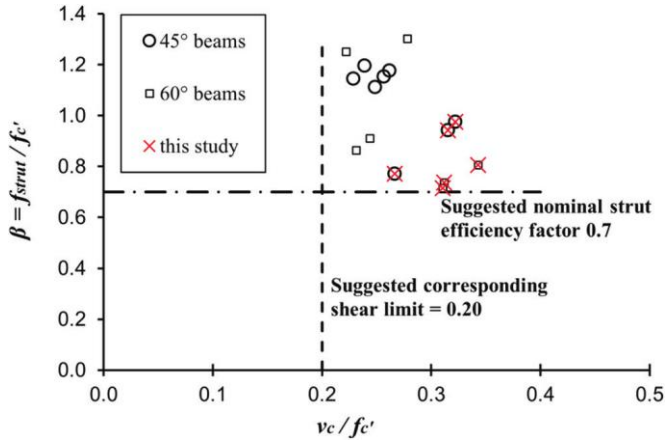

Figure 36: Relationship of strut efficiency factor and normalized shear stress

The authors suggested following equation:

$$For \frac{a}{d} \leq 1, v_{c\ proposed} = v_{c\ strut} = 0.20 * f'_c$$

They also suggested following equations for other a/d ratios, regarding the generic shear enhancement factor:

$$for\ 1 < \frac{a}{d} \leq 2, v_{c\ proposed} = (v_{c\ strut} - v_{c\ code})\left(1 - \frac{a}{d}\right) + v_{c\ strut}$$

$$for\ \frac{a}{d} > 2, v_c = v_{c\ code}$$

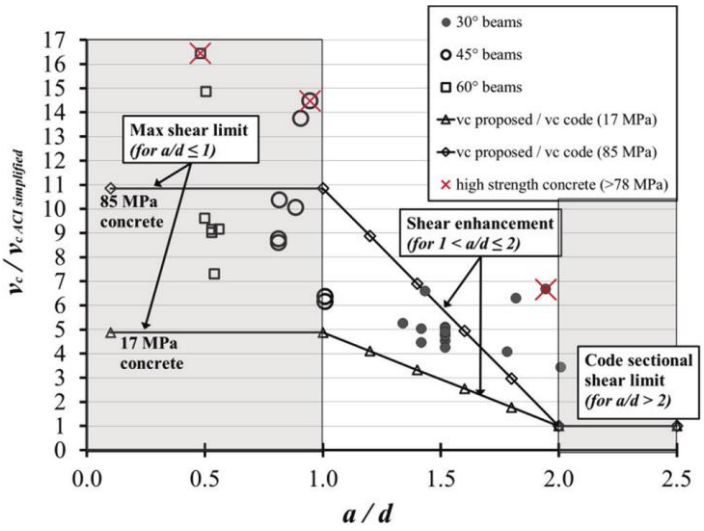

Figure 37: Proposed unified shear stress limit model with the aforementioned equations

3.2.7.2 Discussion

An improvement to the codes, specifically to the ACI 318, was to change the nominal unreinforced strut efficiency factor from 0.6 to 0.7. They also stated that the use of a constant value for the nominal unreinforced strut efficiency factor was the best option instead of calculations, as used in some code provisions.

After consulting ACI 318-14, we came to the conclusion that this factor isn't changed. This could be because of several reasons, first off all they are waiting on more research regarding the subject to evaluate and implement the proposed unreinforced strut efficiency factor in the codes. On the other hand the code provisions need to be general applicable to all kinds of deep beams (other a/d values, different kinds of reinforcement, openings, no openings, different concrete strength, strut angles etc.) and therefore they first need to be sure that the proposed factor is applicable to every deep beam designed with the code provisions and not only to the 9 specimens the researchers tested. But we think, considering the already relatively conservative nature of the ACI 318-11 code (AVG of 1.58 and COV of 0.18), that it's highly likeable that the proposed factor can be implemented and used in the ACI code and we trust in

the authors that they did a good recommendation. In other codes they still use formulas to calculate the effective unreinforced strut efficiency factor.

Regarding the graphical presentation in figure 36, we think that is safe to say that the proposed equation for the maximum shear limit could be viable to use and could be easily implemented in the codes. The authors also stated that they used different strut angles and also high strength concrete and came to the conclusion that the limits are applicable to a wide range of concrete strengths and strut angles. After looking up ACI 318-14 code we couldn't find the adopted measure and therefore it is not used in the code. The cause is probably the same as before mentioned that to implement such limit it needs more testing and research with a wide range of different kind of deep beams.

The authors stated that this suggestion for the maximum shear limit can also be used for other elements with a lower a/d ratio, such as transfer girder, pile caps and corbels. We think that this suggestion about directly implementing it to use in designing other elements with a lower than one a/d ratio is rather substantiated. This is because, even if aforementioned elements are all D-regions, you can't just say the rule is also applicable to those elements. Because these elements maybe have other responses, stresses or conditions compared to deep beams. To make this applicable to those elements further researched should be done by the authors or other researchers.

They also proposed other equations concerning a/d ratio between one and two, and for an a/d ratio higher than two. A generic linear shear enhancement factor was suggested for an a/d ratio between one and two, to bridge the gap between the ultimate shear limit of the STM and the sectional shear stress limit. Because it's linear it could be derived using figure 37. This equation was not experimentally validated but rather derived from a linear line between the STM limit and sectional shear stress limit. Therefore it's advisable to use this limit with caution.

For an a/d ratio above two, the limit stayed the same as in the code.

3.2.8 Strut efficiency-based design for concrete deep beams reinforced with fiber-reinforced polymer bars

In this paper (Mohamed et al., 2016), the authors proposed a strut-and-tie model to predict the shear strength of fiber-reinforced polymer (FRP) reinforced deep beams. By comparing different code provisions, the ACI 318-11 and CSA S806 (2012), they identified the most important parameters affecting the strut efficiency factor. After the conclusion that the STM

models from the codes don't represent the capacity of the FRP-reinforced deep beams well enough, they introduced their own proposal for a strut efficiency factor β_s.

3.2.8.1 Outline of research

They tested 12 specimens of their own, having an a/d of 1.47, 1.13 and 0.83. As mentioned above they used a strut-and-tie model to design these D-regions. The specimens with no vertical web reinforcement used a one-panel STM while the four specimens with vertical web reinforcement used a two-panel STM. This is shown in figure 38 and 39. The two-panel STM was only implemented after they checked the strain-energy ratio. If the strain-energy ratio is less than one, than a single-panel STM used. If it's higher than one, than a two-panel STM is used.

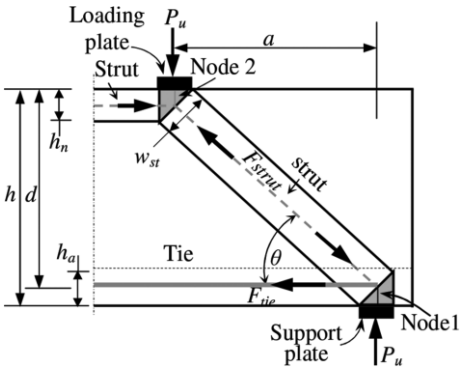

Figure 38: Single-panel STM

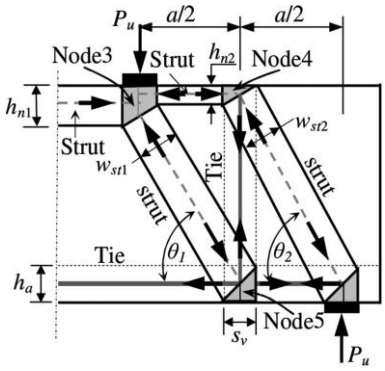

Figure 39: Two-panel STM

The predicted capacity using ACI 318-11 was overestimated. This could be the result of the neglect in the code of the concrete softening in the diagonal strut because of the presence of a high strains in the longitudinal reinforcement. On the other hand in the CSA S806 (2012) the effect of concrete softening was exaggerated, causing a big underestimation of the capacity.

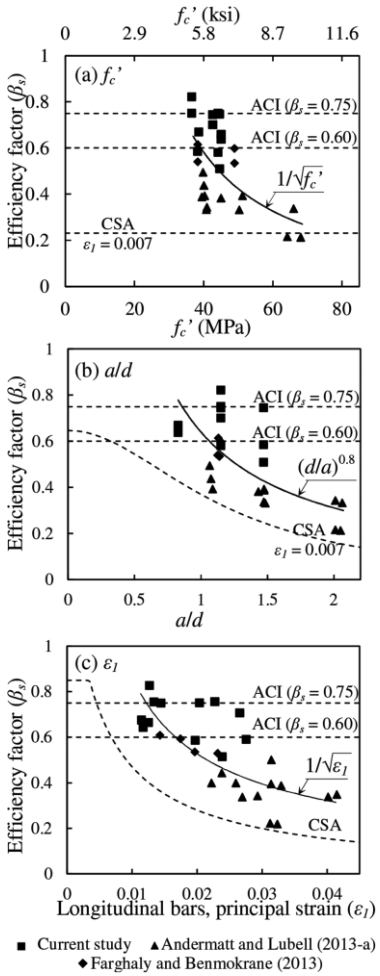

Figure 40: Factors affecting the measured efficiency factor

According to the authors the principal tensile strains ε_1 is more related to the efficiency factor β_s than the strain of the longitudinal bars. Using three parameters (figure 40), the concrete compressive strength, shear span-depth ratio and the principal tensile strains, they were able to propose following equation for the efficiency factor of FRP reinforced deep beams:

$$\beta_s = z * \left(f'_c\right)^a * \left(\frac{a}{d}\right)^b * (\varepsilon_1)^c$$

In this equation z is a constant and a, b and c are constants that represents the correlation between the above mentioned parameters and β_s. They performed least-squares regression on the test results to identify the correlation of the parameters. They obtained following values for a, b and c: -0.5, -0.8 and -0.5 respectively. The constant z was set to 0.5, that way they have an estimation in the lower limit of the data. f_c' is the concrete compressive strength and a/d is the shear span-depth ratio. ε_1 was calculated using following equation:

$$\varepsilon_1 = \varepsilon_{frp} + \left(\varepsilon_{frp} + 0.002\right) * cot^2\theta$$

ε_{frp} is the tensile strain in the tie bar positioned closest to the tension face in the deep beam and has angle θ to the strut axis.

FRP reinforcement performs linearly, that way maximum stresses and strains can be calculated using the force acting on the tie and the elastic modulus E_{frp} of the used bar. The proposed truss model predicts the capacity fairly well with an average of 1.17 and a COV of 15% (figure 41).

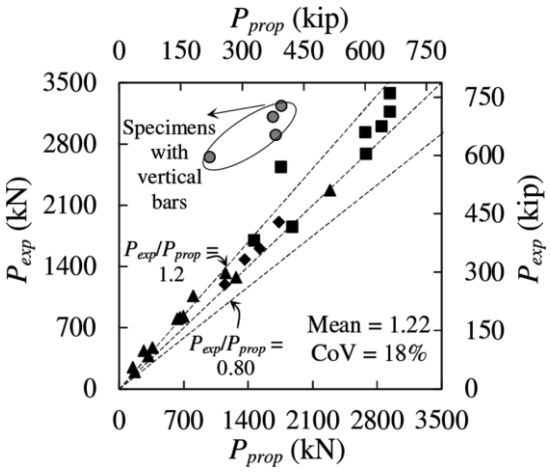

Figure 41: The experimental strength versus the estimated strength

Using the proposed model for FRP reinforced deep beams on steel reinforced deep beams gave rather well predictions as well with an average of 1.09 and a COV of 22% (figure 42). Comparing this to ACI 318-11 and CSA S806 (2012), you could say the proposed model did rather well. ACI overestimated the capacity while CSA underestimated the capacity.

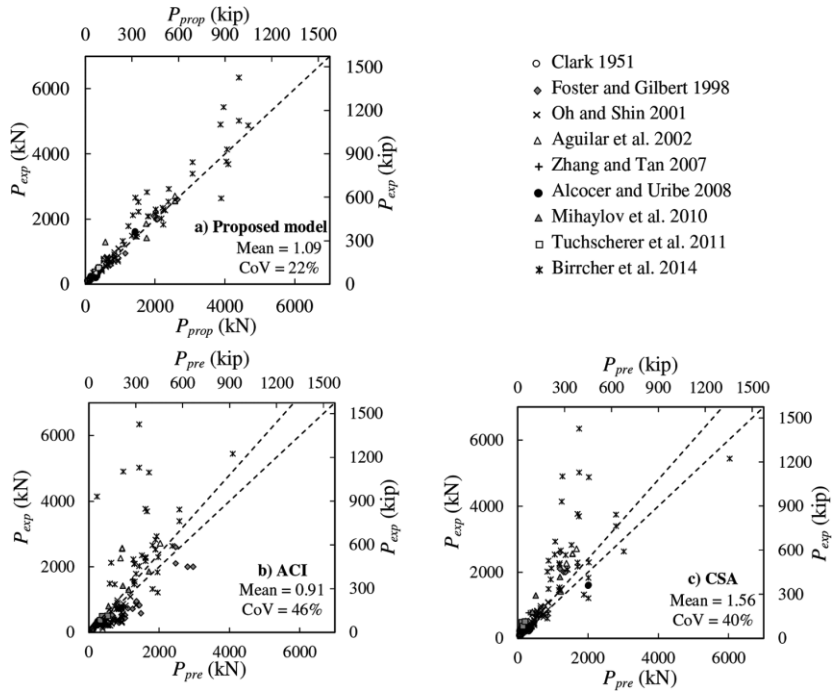

Figure 42: Experimental results of applying the proposed model to steel reinforced deep beams

Even if the authors used a two-panel STM for the specimens with vertical web reinforcement, they still advise to use a one-panel STM because it still results an satisfactory level of conservatism.

3.2.8.2 Discussion

The authors don't say it's applicable to all deep beams, they just say that the proposed model is rather accurate and not too conservative to be used on the kind of deep beams they tested, ranging from an a/d ratio between 0.83 to 1.47. The results of the strength predictions were an average of 1.17 and a coefficient of variation of 15% (figure 41). If the proposed model were to be used on deep beams with an a/d of 2.00 for example, the results could maybe be not so favourable. Therefore this could be a good subject to research in the future. They also tested the model on steel reinforced deep beams and it resulted in rather good results with an AVG of 1.09 and a COV of 22% (figure 42), it is very good to know that the model is also applicable for deep beams with steel reinforcement. Because the proposed strut efficiency factor delivered good results for both kind of deep beams tested, it could be a step in the right direction regarding a general equation for both steel reinforced and FRP reinforced deep beams.

The only limitation of the equation we could think of, is the fact that the factors for the correlation between the parameters is derived from the test results. To solve this problem, there should be done a lot of statistical analysis on a lot tests specimens to find a constant value that can be

used by everyone. For example, a building company don't want to do a statistical analysis of some results, they just want to look up a code provision and use the value described in there. Also regarding the constant value of z, there should be a lot more research to determine a general value of z that could be used in the codes.

Our conclusion is that the model with the proposed strut efficiency factor delivers rather accurate and correct results for both steel reinforced and FRP reinforced deep beams, however the correlation parameters and the parameter z should be further investigated to try and find constant values or values that are not derived from statistical analysis.

3.2.9 Experimental investigation on continuous reinforced SCC deep beams and comparisons with code provisions and models

The aim of this paper (Khatab et al., 2017) was to experimentally investigate the behaviour of self-compacting concrete (SCC) deep beams. The main parameters that were investigated are the shear span-depth ratio, the amount and configuration of web reinforcement and longitudinal reinforcement. The shear predictions from three major codes EC2, ACI 318-11 and CSA23 are evaluated as well is the STM predictions from these codes.

3.2.9.1 Outline of the research

The model to evaluate the applicability of different STM provisions for continuous deep beams is a simple single strut-and-tie model for both the shear span-depth ratios (0.8 and 1.7) and can be seen in figure 43.

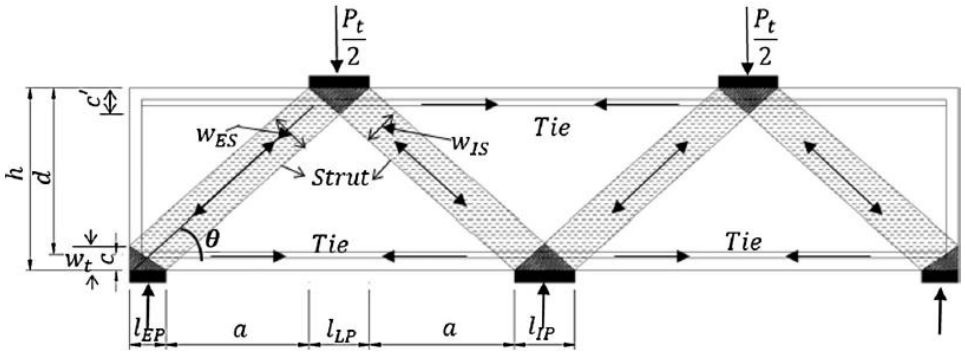

Fig. 9. Schematic STM for continuous deep beams.[16]

Figure 43: The simple single strut-and-tie model that's used

The authors do not propose modifications on the STM models but present some remarkable conclusions based on their tests for continuous deep beams. The other main observations are

not related to the use of STM, but give some useful insights for the construction of continuous deep beams.

Observations:

- The size effect (considering b and h) has almost no influence on the shear strength because of the use of web reinforcement. The shear strength was most influenced by the concrete compressive strength. Moreover the influence of vertical web reinforcement had more influence than horizontal web reinforcement on the capacity.
- Regarding the deflections of the beams in mid-span, all of the beams showed low ductility at failure and this wasn't influenced by the shear span-depth ratio. This is remarkable because this is not the matter with normal concrete deep beams that are tested by other authors.
- Vertical web reinforcement yielded prior to the horizontal web reinforcement in the other group of specimen. From this the authors could correctly conclude that vertical web reinforcement is more effective than the horizontal.
- All predictions according to the three investigated STM provisions were observed as conservative for the SCC deep beams. ACI STM prediction was the best one among the three code provisions.

3.2.9.2 Discussion

This study is one of the first experimental studies performed on continuous SCC deep beams. In current codes there is no specific section describing guidelines for design continuous deep beams according to STM with this kind of concrete. These studies are always of interest because it tests broadening the range of applicability of STM to new structures. Self-compacting concrete is being used more and more nowadays. SCC gives higher quality to structures, improves productivity and gives structural properties to a structure similar to normal concrete. We conclude that there is a high significance for such researches.

The most important experimental observation related to the use of STM for these kind of structures is the influence of different kinds of web reinforcement. The strut-and-tie method recommends the use of web reinforcement crossing concrete struts. They give no suggestions on the web reinforcement being horizontal or vertical. Similar tests have been conducted in the past on continuous deep beams with normal concrete and for these members it was shown that if a/d>1 (shear span-depth ratio) vertical web reinforcement was more effective and

otherwise horizontal reinforcement. The tests conducted in this study showed similar results. For the considered shear span-depth ratio it was shown that vertical web reinforcement is more effective than horizontal web reinforcement. The limitation of this study is the low amount of experimental tests, so it is impossible to generalize this to all SCC continuous deep beams. However, similar studies could be done on a larger database of beams, providing stronger argumentations to adopt proposals considering the layout of web reinforcement into codes of practice.

Overall, different STM predictions were compared for strength predictions on SCC continuous deep beams. It is an interesting observation that ACI could predict the strength the best of the three major codes. The only difference between the codes used in this STM predictions was the concrete effectiveness factor. We can't really conclude why ACI gave the best predictions only based on this factor. Further research is necessary to develop the code provisions on this specific concrete member. However, at this point and with the scarce research that has been conducted on this structural member, we suggest the use of ACI STM to designers.

3.2.10 Shear behaviour of reinforced concrete deep beams

In this paper by Ismail et al. (2017) the parameters affecting the shear capacity are researched, these parameters include the shear span-depth ratio, concrete compressive strength, web reinforcement ratio, and effective beam depth. This was done by experimental testing and they came to the conclusion that the concrete compressive strength and shear span-depth ratio were the most influential for the shear capacity of a concrete deep beam. This was then compared to code provisions and came to the conclusion that following the ACI 318-14 the predictions were conservative for normal-strength concrete but became more unconservative when moving over to high-strength concrete. The EC2 was generally conservative but became more unconservative when using higher concrete strengths.

3.2.10.1 Outline of the research

The authors used a strut-and-tie model to design the deep beam. The STM model seen in figure 44 shows the strut-and-tie layout and also defines the size of each element. Code provisions give the user of STM information about the allowable stresses but not about the size of the strut-and-tie elements. Therefore the authors need to rely on arbitrary decisions to define the size of the strut-and-tie elements.

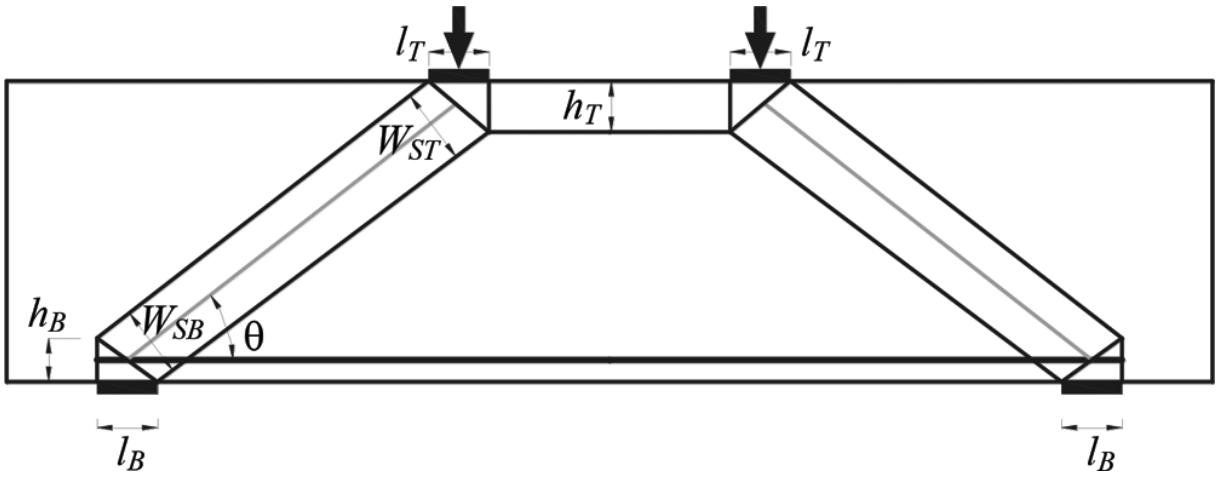

Figure 44: The used strut-and-tie model

There were 24 reinforced concrete deep beams tested with different parameters. The shear span-depth ratio was 1.67, 1.29 and 0.91, the concrete compressive strength ranged from 30 to 85 MPa, the amount of skin reinforcement ranged from 0 to 0.215% and the vertical shear reinforcement ranged from 0 to 1.26%.

The effect of the shear span-depth ratio is that the shear capacity increases when the a/d ratio is decreased. This is mainly because of the fact that when decreasing the a/d ratio, the load is transferred via a direct single strut. On this matter the ACI 318-14 is generally unconservative while the EC2 is results in conservative results. In both cases, when increasing the a/d ratio, the results are less conservative. This is caused by the fact that the codes only account for the a/d ratio through a change in the angle of the inclined strut, that in turn changes the width of the strut. The codes don't account for any concrete strength decrease of the strut. AASHTO LRFD has generally conservative results but unconservative when the a/d ratio is lower than one but they do account for the strength decrease in the effectiveness factor v' but they don't do it properly.

The effect of concrete compressive strength is that the shear capacity increases with an increase in compressive strength and is even more pronounced with beams with lower a/d ratios. Both ACI 318-14 and AASHTO LRFD become more conservative when increasing in concrete compressive strength. This is because they don't adept for the change in concrete compressive strength in the effectiveness factor of the inclined strut. While the EC2 does account for the effect of the concrete compressive strength, it has a more accurate and generally conservative estimates.

Vertical shear reinforcement can lead to an increase of 20% in load capacity because this kind of reinforcement can directly transfer a portion of the applied shear force to the support. Skin

reinforcement is more effective in deep beams with an a/d ratio lower than one. By using skin and vertical reinforcement, shear resistance of concrete is increased because of a phenomenon called aggregate interlock, this results in a reduction of the crack opening in the specimens. Deep beams with higher a/d tends to have more benefits when using conventional vertical web reinforcement. The level of safety of ACI 318-14 code doesn't differ much because the shear reinforcement doesn't have a big impact on the shear strength. The reason behind the unconservative results of ACI 318-14 is that they don't account for the influence of shear span-depth ratio and concrete compressive strength. AASHTO LRFD and EC2 are conservative for deep beams with shear reinforcement, but without shear reinforcement they are rather unconservative. This is because these codes don't adept for the influence of shear reinforcement in the effectiveness factor, therefore having a unconservative estimation of this factor concerning deep beams without shear reinforcement.

In general the codes don't adept for the change in size of the specimens in their formulas to calculate the shear capacity. However it does have an effect on the shear capacity.

3.2.10.2 Discussion

The authors didn't really suggest some improvements to the codes but rather compared different codes concerning the shear capacity of reinforced deep beams. They identified whether codes were conservative or unconservative towards different parameters that influence the shear capacity, these were the shear span-depth ratio, concrete compressive strength, size effect and vertical and skin reinforcement. Some of the parameters are taken into consideration but sometimes not done well or through the effectiveness factor v'. All of these parameters should be taken properly into consideration when designing deep beams.

The effectiveness factor v' was also studied. The concrete compressive strength had the biggest influence, also the shear span-depth ratio and shear reinforcement have an effect on the factor (figure 45), however the impact of the size effect was not studied in this paper. None of these parameters are all accounted for in any code when calculating the effectiveness factor v'. Therefore it's our suggestion that the codes should determine an effectiveness factor that includes the shear span-depth ratio, the concrete compressive strength, size effect and skin and vertical shear reinforcement because these are the parameters that influence the shear capacity of a deep beam the most. Some codes implement one or two parameters and some implement it and do it wrong.

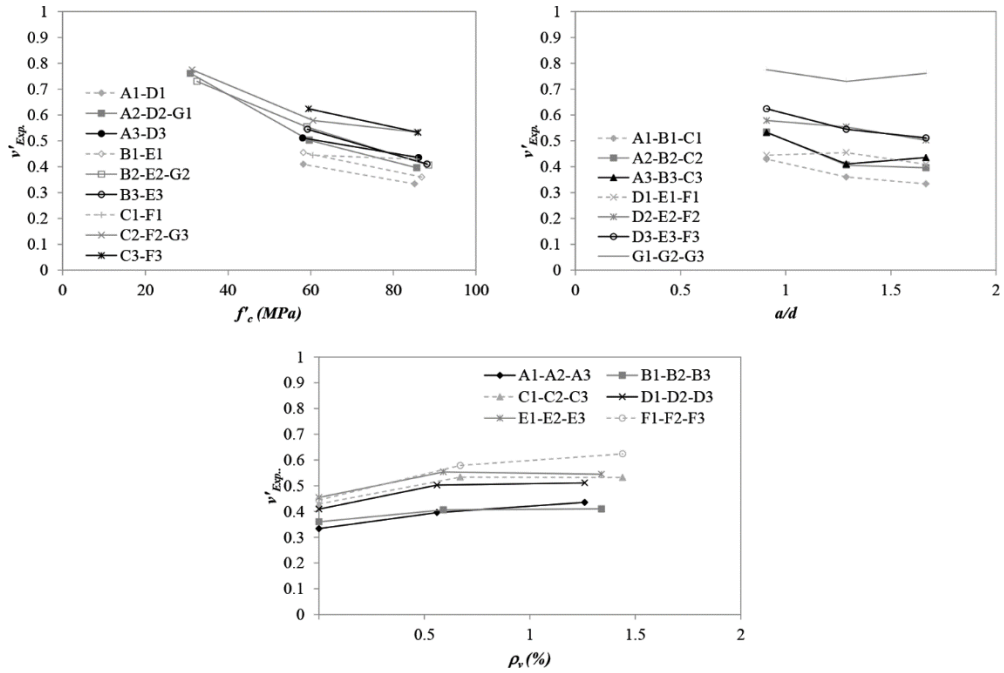

Figure 45: Influence of different parameters on the strut effectiveness factor

An effectiveness factor v' that includes all aforementioned parameters could lead to conservative and accurate shear capacity predictions for all kinds of deep beams and could be implemented in all code provisions to have better designs.

3.2.11 Shear strength prediction of reinforced concrete deep beams with web openings

In this paper by Tseng et al. (2017) an analytical method is presented to predict the shear strength and evaluate the failure mode and its position of reinforced concrete deep beams with openings. Using a strut-and-tie approach, the authors aimed to define the shear-transfer path. The distribution of the shears above and below the web opening is based on the stiffness ratios. The proposed model was rather rational concerning the shear strength predictions and has significant physical configurations. This was done with simple calculations and therefore it could be appropriate for engineering applications.

3.2.11.1 Outline of the research

The proposed model initiates with defining the shear transfer paths and shear stiffness ratios. With these two parameters the shear strength can be determined by implementing the equilibrium and the constitutive laws of the materials in this method.

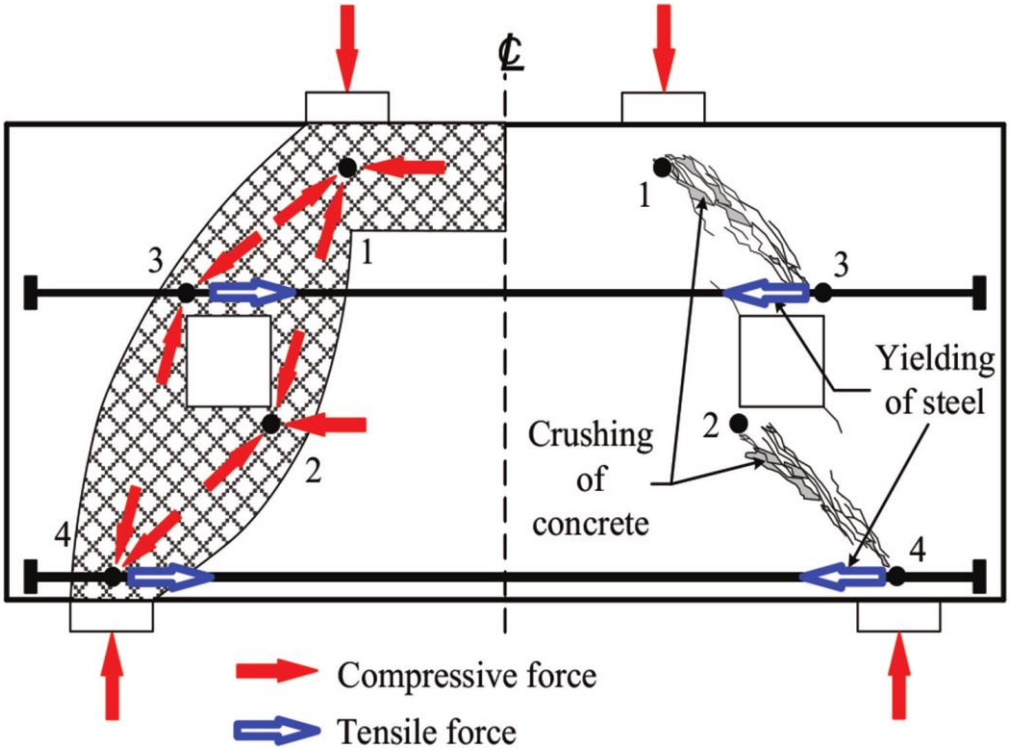

Figure 46: Proposed model with the location of the nodes and the shear transfer path

The shear-transfer path of the proposed model is shown in figure 46. As you can see, there are two paths for the shear to follow, resulting in four nodes. The shear stresses are assumed to be transferred completely through the compressive struts. When using a strut-and-tie model it's important to define the positions of the four nodes. The full explanation of the position of these nodes can be found in the paper itself. Using following figure 47, the node positions can be determined. The full explanation of the position of the different nodes can be found in the paper itself.

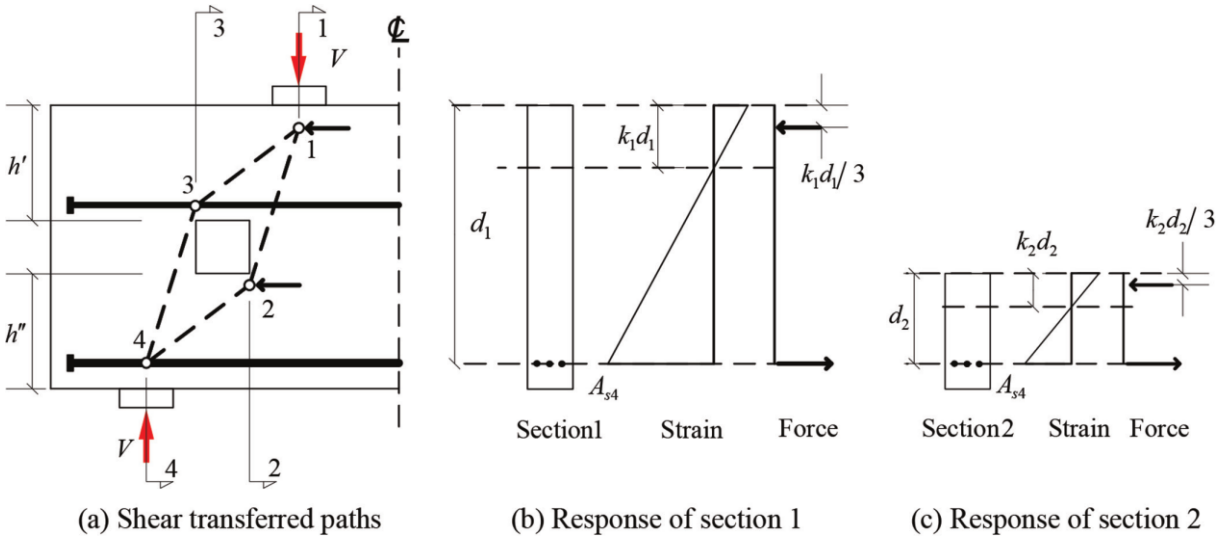

Figure 47: Location of the nodes

An important parameter to determine the position of the nodes is the depth of the compression zone. This parameter can be calculated following next equation:

$$kd = \left(\sqrt{\left(n * \frac{A_s}{b * d} \right)^2 + 2 * n * \frac{A_s}{b * d}} - n * \frac{A_s}{b * d} \right) * d$$

- d is the effective depth of the deep beam.
- b is the width of the deep beam.
- n is the ratio of the elastic modulus of the reinforcement vs elastic modulus of the concrete ($n = E_s/E_c$).
- A_s is the total cross-sectional area of the flexural reinforcement in the deep beam.

In the deep beam there are two sections, therefore k_1d_1 and k_2d_2 represent each section respectively.

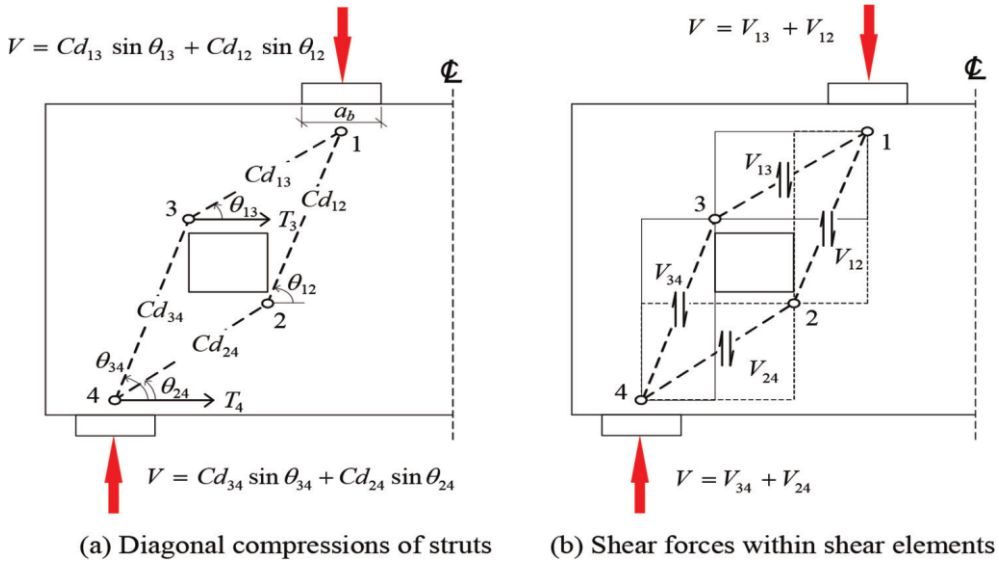

Figure 48: Force and shear distribution among loading paths

Figure 48.a shows the internal force distribution of the proposed model and figure 48.b shows the shear element of each individual compressive strut. The shear of one element can be calculated if the shear stress is uniformly distributed and the shear stress τ and shear strain γ meets Hooke's law:

$$V = b * y * \tau = b * y * G * \gamma$$

With y the height of the shear element, G the shear modulus. Shear deformation Δ can be calculated using following equation:

$$\Delta = x * \gamma$$

In this equation x represents the length of the shear element. Using these two equations the shear stiffness factor k can be obtained.

$$k = \frac{V}{\Delta} = \frac{b * y * G * \gamma}{x * \gamma} = \frac{G * b * y}{x} = G * b * \tan\theta$$

Θ is the angle of the shear element its diagonal with the horizontal axis. The shear stiffness factor of one shear element can now be calculated, the next step is to calculate the shear stiffness factor of a whole shear path. This can be done by using the stiffness rule of springs connected in series (figure 49).

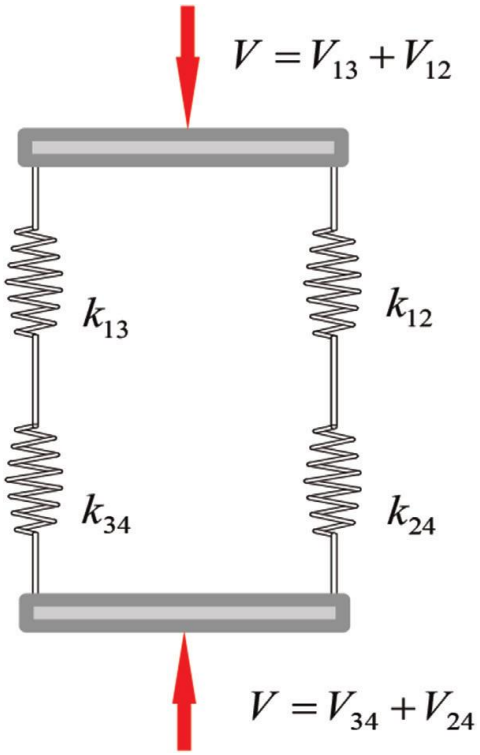

Figure 49: Stiffness simulation of loading paths

The equations to calculate the shear stiffness factor of the two shear paths are now given:

$$k_{134} = \frac{1}{\frac{1}{k_{13}} + \frac{1}{k_{34}}}$$

$$k_{124} = \frac{1}{\frac{1}{k_{12}} + \frac{1}{k_{24}}}$$

Where k_{ij} is the stiffness of the shear element ij.

At last the shear force distribution can be determined using the above mentioned equations, resulting in next equation:

$$\frac{V_{134}}{V_{124}} = \frac{V_{13}}{V_{12}} = \frac{V_{34}}{V_{24}} = \frac{k_{134}}{k_{124}} = \frac{\frac{tan\,\theta_{13} * tan\,\theta_{34}}{tan\,\theta_{13} + tan\,\theta_{34}}}{\frac{tan\,\theta_{12} * tan\,\theta_{24}}{tan\,\theta_{12} + tan\,\theta_{24}}}$$

They experimentally tested this on their own specimens. They divided those in two groups: Type A and Type B. Type A are the specimens that have horizontal tensile reinforcement above the web opening while Type B are the ones without this kind of reinforcement. For Type A specimens the average (AVG) of the experimental versus the predicted value is 1.30 with a coefficient of variation (COV) of 6%, While Type B specimens had an AVG of 1.34 and a COV of 18%.

To enhance the shear strength of a deep beam with web openings the authors proposed a formula to determine the percentage of horizontal reinforcement that needs to be added above the web opening. The equation can be obtained if assumed that the installed reinforcement above the web opening have as much tensile splitting strength as the concrete surrounding it and is described as:

$$\rho_{h,13} = \frac{f_r}{f_{yh}}$$

- f_{yh} is the yield strength of the steel
- f_r is the modulus of rupture of the concrete and can be calculated using following equation: $f_r = 0.62 * \sqrt{f'_c}$ [MPa]

The percentage of improved shear strength in the deep beam ranges from 3 to 39%.

3.2.11.2 Discussion

First of all, we think it is very logical to use horizontal tensile reinforcement above a web opening in a deep beam because there are always tensile forces above an opening in a concrete element. Our reasoning behind this is that we have learned to always put at least a minimum amount of horizontal tensile reinforcement above an opening in a reinforced concrete element, such as walls, beams, plates etc. As the authors investigated this in their study and determined a formula to calculate this kind of reinforcement in deep beams, we are drawn towards believing

them that this is a viable and correct option. This formula was a simple one and could be easily calculated. Because of this ease, it could be implemented in code provisions.

Regarding their proposed model and their comparison with other models, it is safe to say that they developed a rather conservative but accurate model. The model had an average value of 1.30 and a low coefficient of variation of 6% for specimens A and an average value of 1.34 and a coefficient of variation of 18% for specimens B. As illustrated by the numbers the model was certainly very good for the specimens with horizontal reinforcement above the web opening of the deep beam (Type A specimens). They also presented a way to calculate the positions of the nodes, this is very good because the location of the nodes are very important in a strut-and-tie model. The parameters used were easy to determine. However it's a rather specific model to be able to implement it in code provisions.

The way of calculation was rather difficult to understand in the paper itself but with a calculation example added in the appendix, it wasn't that difficult to follow and understand.

3.2.12 Strut-and-tie modelling of reinforced concrete deep beams

The aim of this paper by Ismail et al. (2018) is to develop a unified procedure for using STM for the design and analysis of RC deep beams. The main factor that is investigated is the formulation of the concrete effectiveness factor used to account for the biaxial state of stresses in the struts of deep beams. A new effectiveness factor is proposed and evaluated by experiments and compared with the existing factors that are described in current codes.

3.2.12.1 Outline of the research

For simplicity, two simple STM models were adopted in the beginning of this study. The first one is a single strut-and-tie model (used for a/d<1) and a truss model (used for 1<a/d<2). The authors assessed the ability of these models for developing enhanced equations and concluded that the single strut-and-tie model gave the best strength predictions. This model was further used in the study, see figure 50.

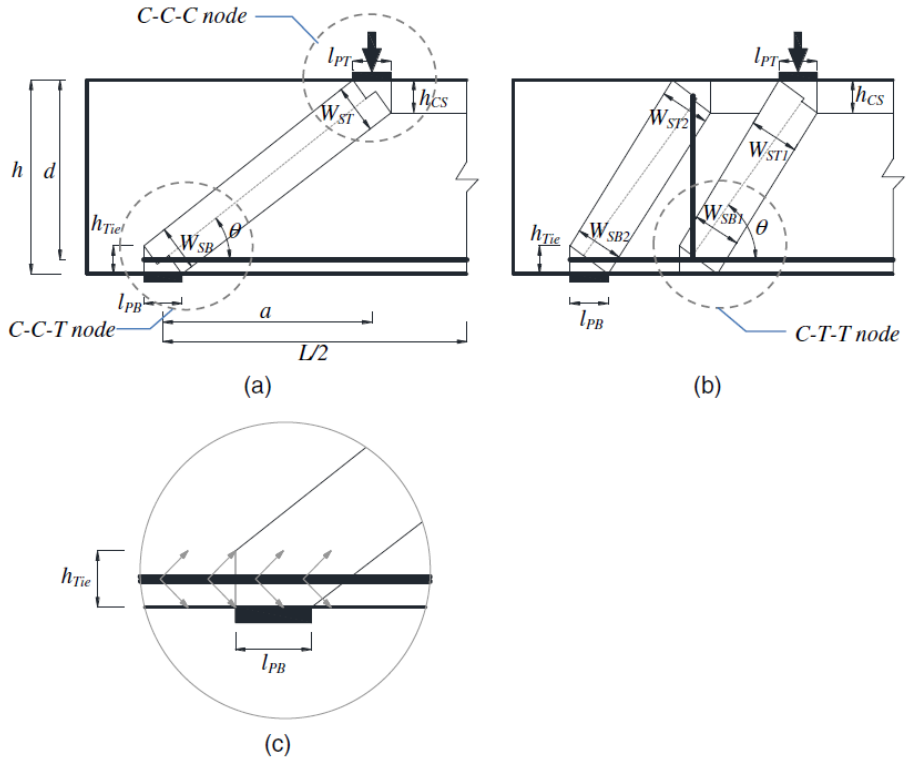

Fig. 1. Load transfer mechanism in RC deep beams: (a) strut-and-tie model; (b) truss model; (c) height of the bottom node

Figure 50: Different load transfer mechanism in RC deep beams (In this paper, mechanism a) is used)

Eight existing approaches and formulations on the effectiveness factor are experimentally evaluated first using this STM. More details on them can be found in the article. Based on the average shear prediction effectiveness some main conclusions could already been made to take into account for the proposed factor.

The ultimate proposed effectiveness factor is a simplification of the ratio between the compressive strength of a concrete specimen subjected to lateral tensile strain by Bazant and Xiang (1997) and the uniaxial strength of the concrete (f_c):

$$\nu = \alpha \sqrt{\frac{2EG_f}{W_s \varepsilon_1}} \Big/ f_c$$

3.2.12.2 Discussion

The factors E and G_f are respectively the modulus of elasticity and the fracture energy of concrete, which can be both easily calculated using code prescriptions. W_s represents the width of the strut.

Factor ε_1 represents the lateral tensile strain. The main factors influencing the tensile strain are shown to be the effective depth and the shear-span to depth ratio based on the authors finite-element analysis. This resulted in the following equation, which is based on best fit analysis:

$$\varepsilon_1 = 0.02 \frac{(\frac{a}{d})^{0.5}}{(\frac{d}{150})^{0.35}}$$

Comparison with finite-element again proved that this equation leads to a reasonable prediction of the tensile strain in the shear span of RC deep beams. We can remark that this equation is highly dependent on the quality of the finite-element model that was used.

The factor α is a calibration factor that is implemented because of the simplification that is introduced to use the tensile strain, which is earlier described, with the experimental date of crack properties. An average is determined from experimental and numerical data. A value of 400 and 450 was derived respectively for deep beams without and with shear reinforcement to account for the effect of this factor. For simplicity reasons in codes of practice, this seems to be a proper way to implement in those codes.

Considering the node strength factor, the paper uses no reduction of the uniaxial compressive strength of concrete compared to the codes which uses reduction factors for the CCT node. They based this assumption on the observation that there were no cracks in this nodal zone, which means that the tensile stress was always below the concrete tensile stress. To us it seems unconservative to conclude this just based on some visual inspections on a limited database of experiments.

CCC node factor can be greater than 1 following codes because of confinement but here they use 1 to remain conservative. The arguments the authors use is the uncertainty of triaxial confinement when the deep beam is loaded by a column instead of bearing plates. We think the authors are not being consequent when considering conservativeness or not for these node factors. Therefore we won't follow their reasoning and we suggest to use of current node strength factors from the codes. It has also been well reported that multiaxial concrete reaches up to three times the uniaxial strength of concrete, so higher factor could be also applied.

The proposed model with the new concrete effectiveness factor is experimentally evaluated and compared with the provisions from other authors and codes. Results show that the proposed model can predict the capacity less conservative and with lower scatter. After applying safety factors it is the only model which gives 100% safe predictions for the presented

database and still with the lowest averages as seen in figure 51. It is also demonstrated in figure 52 that the proposed model captures the effect of shear span-depth ratio, concrete compressive strength and effective depth better than current codes do. When varying these three parameters the proposed model is able to keep a more horizontal trendline which indicates that the factors are better implemented in the formulation of the concrete effectiveness factor.

Table 2. Percent of Safe Shear Strength Prediction by STM after Application of Safety Factors

	Beams without shear reinforcement (295 beams)			Beams with shear reinforcement (224 beams)		
Effectiveness factor	Safe prediction (%)	Mean of safe results	Mean of unsafe results	Safe prediction (%)	Mean of safe results	Mean of unsafe results
Marti (1985)	88.3	1.93	0.86	99.6	2.28	0.87
Collins and Mitchell (1986)	96.0	2.34	0.90	98.7	1.96	0.92
Vecchio and Collins (1993)	100	3.32	—	99.6	2.97	0.87
Warwick and Foster (1993)	91.0	1.91	0.88	99.6	2.68	0.87
Modified Collins and Mitchell Foster and Gilbert (1996)	97.1	2.53	0.95	99.6	3.21	0.87
EC2	90.9	1.92	0.91	99.6	2.59	0.75
ACI 318-14	79.3	1.76	0.85	93.3	1.95	0.84
Model Code 2010	88.7	1.99	0.88	99.6	2.69	0.79
Proposed	100	1.63	—	100	1.59	—

Figure 51: Comparison between proposed model and different studies

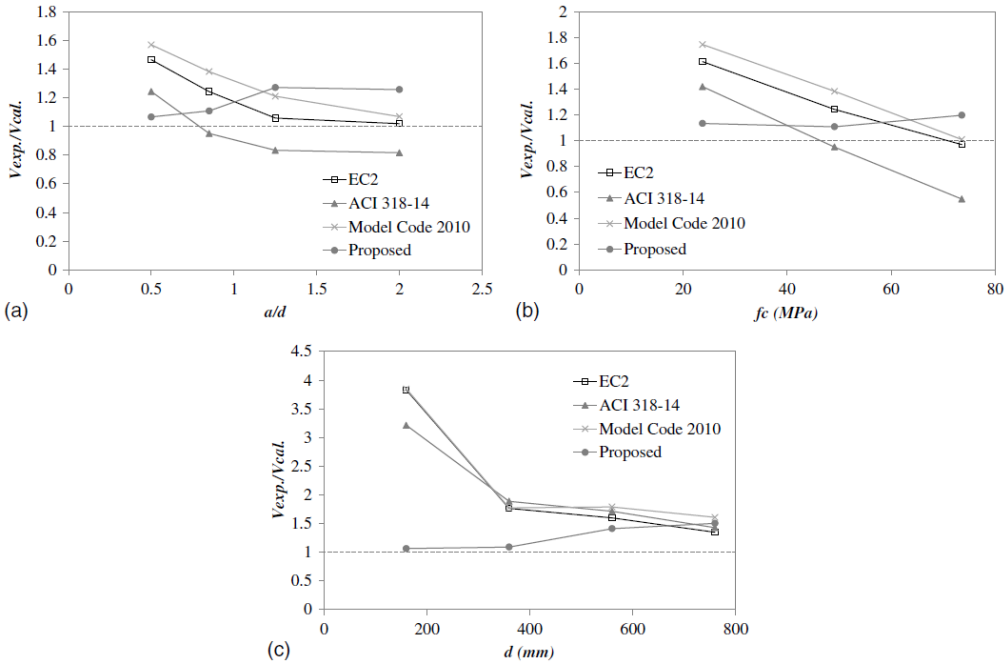

Fig. 12. Effect on performance of different effectiveness factor (with shear reinforcement) of: (a) shear span:depth ratio (data from Oh and Shin 2001); (b) concrete strength (data from Oh and Shin 2001); (c) depth (data from Walraven and Lehwalter 1994)

Figure 52: Influence of different parameters on the effectiveness factor

We can conclude from this experimental data that the proposed formulation is able to give a less conservative and thus economical better prediction of the capacity. The formulation seems solid because it captures all the parameters that are used in different formulations and

combines the effect of them in one equation. The parameters in the equation can be easily calculated and therefore we conclude that it could be adopted in current design codes. The only uncertainty that remains for us to suggest this, is the use of the, for us unknown, finite-element model that is used to define some factors. However, the model is verified against a pretty large database of deep beams and therefore seems to be trustable.

3.2.13 Cracking strut-and-tie model for shear strength evaluation of reinforced concrete deep beams

This study by Chen et al. (2018) presents a new cracking strut-and-tie model. The innovation behind the model is the effect of diagonal cracks on the strength of the inclined strut. The strut is divided into two parts by the critical shear crack, with both parts having different concrete effective strength. Previous and existing STM models in current codes don't take this experimentally observed phenomena of cracks into consideration in their concrete effectiveness factors and consequently causing a higher scatter in their predictions.

3.2.13.1 Outline of the research

The CSTM model that is used is a single-strut model, adopted with a horizontal upper strut because of the four-point bending tests that were performed. The strut is crossed by the critical shear crack with a certain angle as can be seen in figure 53.

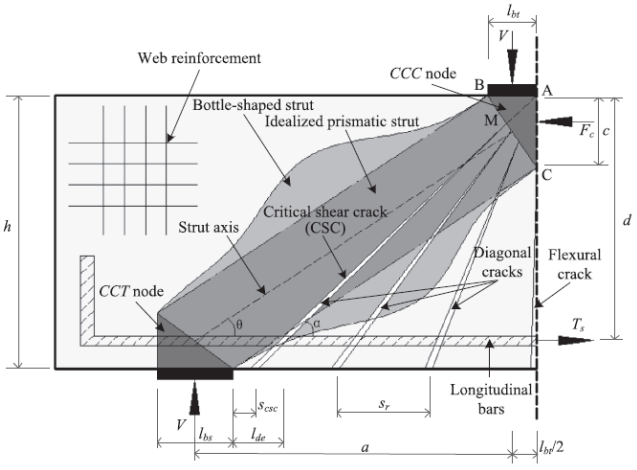

Figure 53: Configuration of strut and cracks of deep beams in CSTM

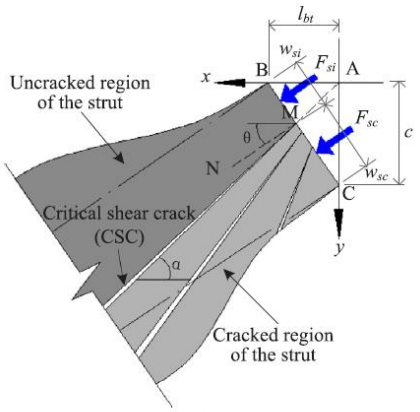

Fig. 4. Strut with diagonal cracks near *CCC* node.

Figure 54: Strut with diagonal cracks near CCC node

The strut is divided by the crossing of the diagonal critical shear crack (CSC), which splits the strut-node interface into two areas as in figure 54. The main idea is that the concrete above the CSC is uncracked and consequently the ultimate compressive strength of the normal bottle-shaped strut can be assumed. The part below CSC is affected by flexural cracks and thus the effective compressive strength should be less. The ultimate forces acting on the node surface in figure 54 are given below:

$$F_{si} = \sigma_{ci} w_{si} b = \kappa_c \beta_{si} f_c' w_{si} b$$

$$F_{sc} = \sigma_{cc} w_{sc} b = \beta_{sc} f_c' w_{sc} b$$

For the uncracked force F_{si}, the effectiveness factor is simply taken by the product of β_{si}=0.85 adopted from Laughery and Pujol (2015) and κ_c=1-f_c'/250 adopted from EC2 (Eurocode 2, 2005).

The innovative part of this formulation is a new approach for defining the equation for the effectiveness factor for the cracked part of the strut:

$$\beta_{sc} = \frac{\sigma_{cc}}{f_c'} = \frac{\sigma_{cc,ag} + \sigma_{cc,s}}{f_c'} \leq \kappa_c \beta_{si}$$

The numerator in this equation accounts for the effects in the cracked part of the strut that transfer the load to the support. They stand respectively for the aggregate interlock action and the sum of dowel action of the longitudinal reinforcement and the tensile strength in web reinforcement.

3.2.13.2 Discussion

First of all, we would like to mention that the paper gives a detailed explanation of the theoretical background on how to calculate the contribution of the aggregate interlock and dowel action. It's not in the scope of this thesis to examine these equations into detail. We would like to refer our readers to the considered paper and we rely on the technical knowledge of the authors to propose their equations.

When we consider the proposed method from a distance, it completely makes sense and can be discussed more easily.

Modulization of the cracked concrete is difficult. The strength of cracked concrete depends on many factors as the amount and position of reinforcement, distance from applied loads, and the pour direction of the concrete.

This model has adopted a very visual description of the effect, two different areas are defined where the critical values are easily calculated. The model accounts for the interlocking effect of aggregates, the dowel action and tensile strength of concrete, all of them fundamentals for a realistic modulization of the concrete plasticity.

We rely and trust on the theoretical background that the authors used for their model. It seems like a more difficult way to use strut-and-tie method but they have managed well to implement their ideas. At the end it all comes down to enhancing the definition of the strut efficiency factor to what happens in experiments.

4 Conclusions

All these papers separately have contributed to enhance the interest in developing of deep beams with strut-and-tie models. Throughout the discussions, it became clear that the STM for deep beams is still not perfect. The strength of deep beams is determined by the shear capacity but shear behaviour is still not well known. Therefore some of the papers focus on this aspect and try to improve the models, formulas, etc. regarding the parameters that have an effect on the shear capacity. Also recommendations for general design, nodal zones and special deep beams are suggested. The focus of this Master Thesis was not to give the best approach or model to design deep beams, as it is with pile caps, but rather to make a collection of the latest recommendations and improvements for deep beams. The discussed papers can somehow be divided into groups considering the kind of recommendations and improvements that were suggested.

A first group discusses some general recommendations and improvements made to the STM of deep beams. Improvement nr. 1 suggested some rules of thumb that can be easily followed when designing deep beams, however they couldn't be implemented into code provisions. Nr. 5 suggested the use of two-parameter kinematic theory to design deep beams. However, with the current interest in STM and the already implementation of STM in the code provisions, it will probably not be used in the future. Nr 6. was an improvement for a smoother transition between the STM and sectional shear design for an a/d ratio around two, for this the authors used the UT STM because it resulted in better predictions. Nr. 7 proposed shear stress limits they extracted from experimental data. These shear stress limits could be easily adopted by code provisions.

A paper also suggested improvements to the nodal zones (Nr. 2). The nodal zones in deep beams were already well known but the authors tried to improve the concrete compressive strength and stress limits in nodal zones. The first suggestion was a proposal of an increasing factor of compressive strength in the nodal zones due to triaxial confinement of concrete around the nodal zone. The second suggestion regarded the stress limits in nodal zones, the most important one was the strut-to-node or strut efficiency factor that changed.

Following the change in strut efficiency factor, a second group of authors gave suggestions to improve the strut efficiency factor. The strut efficiency factor is very important because it is directly related to the shear capacity of a deep beam and this is again related to the strength of

the deep beam itself. One author (nr. 6) just stated that the AASHTO should change the efficiency factor, another one (nr. 7) just changed the value of the nominal strut efficiency factor of the ACI 318-14. The most interesting ones were the improvements nr. 8 and 12, they introduced new formulas to calculate the factor. These formulas included the parameters the authors thought to be the most influential, namely the compressive strength and shear span-depth ratio. Also the shear reinforcement was included but in a different way by each author. By doing this, more accurate and correct results can be obtained. In the current codes, no one uses all three parameters. It would be good for code provisions and future researchers to use such efficiency factors to have more accurate and correct results. Our conclusion, regarding the strut efficiency factor, is that at the moment these are the most important improvements that could be made and even investigated in the future. Because they have such a great impact on the shear capacity of a deep beam.

Nr. 13 also proposed an efficiency factor but for the cracked part of the strut in his cracking strut-and-tie model. By using the aggregate interlock action and the sum of dowel action of the longitudinal reinforcement and the tensile strength in web reinforcement in the efficiency factor, it was able to accurately and safely predict the shear resistance of a deep beam.

Some improvements didn’t belong in any group, these were the ones that discussed special kind of deep beams. Nr. 4 stated that the design according to ACI 318-14 was rather conservative, it also made a suggestion for the best way to locate the position of the upper node. Nr. 9 was a recommendation to design self-compacting concrete (SCC) deep beams according ACI 318-14. This was one of the first to suggest a code to design these kind of deep beams. Nr. 11 was a new approach to design deep beams with web openings. They suggested a way to locate the position of the nodes according to the compression zone in the deep beam and also an easy formula to determine the horizontal reinforcement above the openings.

The use of three-dimensional STM to design deep beams is not touched throughout all the papers that we’ve analysed and discussed. The bi-dimensional STM is capable enough to design deep beams.

To make the recommendations and improvements better understandable a graphical representation is made and can be seen in the figure 55 below.

Overall, our entire table of improvements represent a complete list of the most recent and significant studies on the strut-and-tie modelling of deep beams. All the ideas are explained and discussed and this document can be used for future researchers as a basis to adopt ideas

for their own research. We suggest researchers to keep developing the strut-and-tie modelling of deep beams to minimize discrepancy and eventually to obtain a solid and conservative method to design and calculate deep beams of all kinds correctly.

Nr. 2: see table in 3.2.2.2

Nr. 6: AASHTO should change efficiency factor for non-hydrostatic nodes.

Nr. 7: In the ACI 318, change the nominal unreinforced strut efficiency factor from 0.6 to 0.7.

Nr. 8: $\beta_s = z * \left(f'_c\right)^a * \left(\frac{a}{d}\right)^b * (\varepsilon_1)^c$

Nr. 12: $\nu = \alpha \sqrt{\frac{2EG_f}{W_s \varepsilon_1}} \Big/ f_c$

Nr. 13: Efficiency factor cracked part of the strut: $\beta_{sc} = \frac{\sigma_{cc}}{f'_c} = \frac{\sigma_{cc,ag} + \sigma_{cc,s}}{f'_c} \leq \kappa_c \beta_{si}$

Nr. 2: Factor increased compressive strength nodal zones: $m = \sqrt{A_2/A_1} \leq 2$

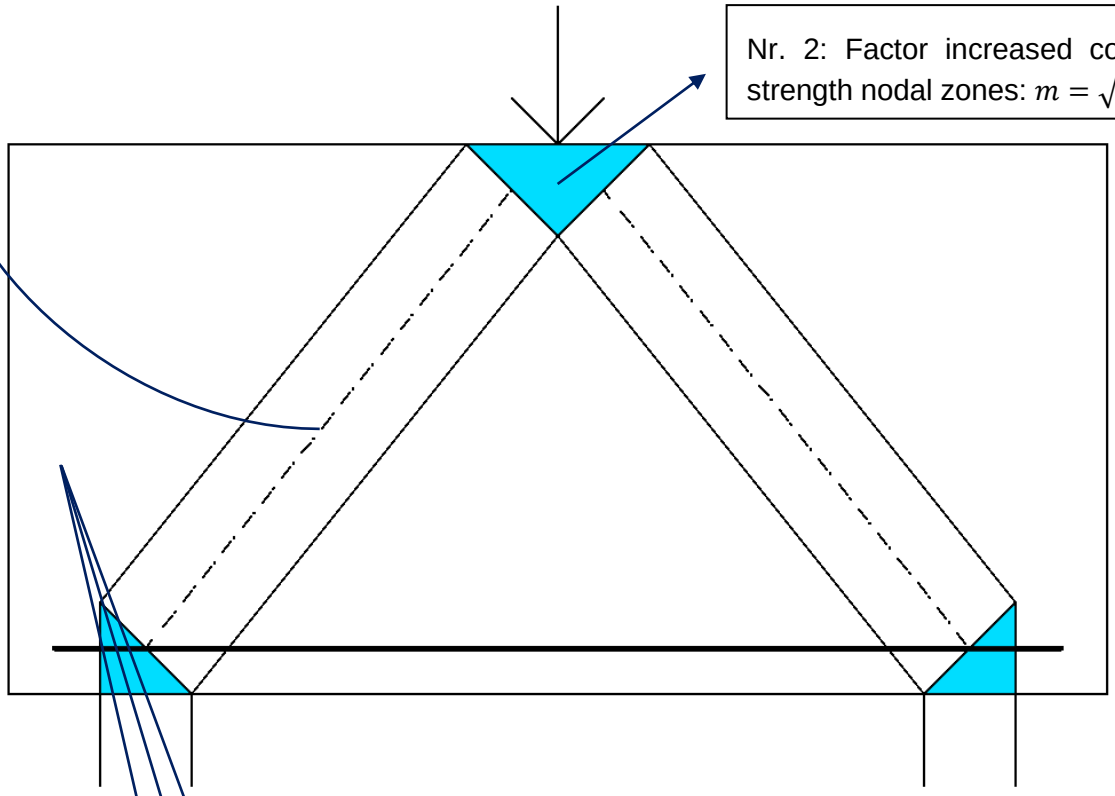

Figure 55: Graphical representation of the most important improvements and recommendations

Nr. 5: The use of 2PKT to design and analyse deep beams

Nr. 6: For a/d between 2.0 and 2.5, recommendation of limiting the ratio of the steel reinforcement to concrete capacity, V_S/V_C to 2.0.

Nr. 7: Shear limits $For\ \frac{a}{d} \leq 1, v_{c\ proposed} = v_{c\ strut} = 0.20 * f'_c$ and $for\ 1 < \frac{a}{d} \leq 2, v_{c\ proposed} = (v_{c\ strut} - v_{c\ code})\left(1 - \frac{a}{d}\right) + v_{c\ strut}$ and $for\ \frac{a}{d} > 2, v_c = v_{c\ code}$

5 List of figures

6 Bibliography

ACI Comittee 318. (2002). *BUILDING CODE REQUIREMENTS FOR STRUCTURAL CONCRETE (ACI 318-02) AND COMMENTARY (ACI 318R-02)*.

ACI Comittee 318. (2014). *BUILDING CODE REQUIREMENTS FOR STRUCTURAL CONCRETE (ACI 318-14) AND COMMENTARY (ACI 318R-14)* (Vol. 11).

American Association of State Highway and Transportation Officials. (2017). *AASHTO LRFD Bridge Design Specifications, 8th Edition*.

Bažant, Z. P., & Xiang, Y. (1997). Size Effect in Compression Fracture: Splitting Crack Band Propagation. *Journal of Engineering Mechanics*, *123*(2), 162–172. https://doi.org/10.1061/(ASCE)0733-9399(1997)123:2(162)

Birrcher, D. B., Tuchscherer, R. G., Huizinga, M., & Bayrak, O. (2014). Depth effect in deep beams. *ACI Structural Journal*, *111*(4), 731–740. https://doi.org/10.14359/51687002

Birrcher, D., Tuchscherer, R., Huizinga, M., Wood, S., Jirsa, J., & Bayrak, O. (2009). Strength and Serviceability Design of Reinforced Concrete Deep Beams. *Technical Report*, *7*(6), 1–400. https://doi.org/10.4028/www.scientific.net/AMR.931-932.473

Brown, M. D., Sankovich, C. L., Bayrak, O., Jirsa, J. O., Breen, J. E., A., & Wood, S. L. (2006). *Examination of the AASHTO LRFD Strut and Tie Specifications*.

Brown, M. D. (2005). *Design for Shear in Reinforced Concrete Using Strut-and-Tie and Sectional Models*. *The University of Texas at Austin*.

Chen, H., Yi, W. J., & Hwang, H. J. (2018). Cracking strut-and-tie model for shear strength evaluation of reinforced concrete deep beams. *Engineering Structures*, *163*(November 2017), 396–408. https://doi.org/10.1016/j.engstruct.2018.02.077

Collins, M. P., & Mitchell, D. (1986). Rational Approach to Shear Design - The 1984 Canadian Code Provisions. *ACI Journal*, *83*(6), 925–933.

El-Sayed, A. K., & Shuraim, A. B. (2015). Size effect on shear resistance of high strength concrete deep beams. *Materials Structural Journal*.

Eurocode 2. (2005). *Eurocode 2: Ontwerp en berekening van betonconstructies - Deel 1-1: Algemene regels en regels voor gebouwen (+AC:2010)*. https://doi.org/10.3403/30206727

Garber, D. B., Gallardo, J. M., Huaco, G. D., Samaras, V. A., & Breen, J. E. (2014). Experimental evaluation of strut-and-tie model of indeterminate deep beam. *ACI Structural Journal*, *111*(4), 873–880. https://doi.org/10.14359/51686738

Ismail, K. S., Guadagnini, M., & Pilakoutas, K. (2017). Shear behavior of reinforced concrete deep beams. *ACI Structural Journal*, *114*(1), 87–99. https://doi.org/10.14359/51689151

Ismail, K. S., Guadagnini, M., & Pilakoutas, K. (2018). Strut-and-Tie Modeling of Reinforced Concrete Deep Beams. *Journal of Structural Engineering*, *144*(2), 04017216. https://doi.org/10.1061/(ASCE)ST.1943-541X.0001974

Khatab, M. A. T., Ashour, A. F., Sheehan, T., & Lam, D. (2017). Experimental investigation on continuous reinforced SCC deep beams and Comparisons with Code provisions and models. *Engineering Structures*, *131*, 264–274. https://doi.org/10.1016/j.engstruct.2016.11.005

Kupfer, H. (1964). Expansion of Morsch's truss analogy by application of the principle of minimum strain energy. *CEB Bulletin*, *40*.

Lambert, P., & Thurlimann, B. (1971). Ultimate Strength and Design of Reinforced Concrete Beams in Torsion and Bending. *Institut Für Baustatik Und Konstruktion*, *42*, 28. https://doi.org/10.1007/978-3-0348-5954-7

Laughery, L., & Pujol, S. (2015). Compressive Strength of Unreinforced Struts. *ACI Structural Journal*, *112*(5), 617–624.

Liu, J., & Mihaylov, B. I. (2016). A comparative study of models for shear strength of reinforced concrete deep beams. *Engineering Structures*, *112*, 81–89. https://doi.org/10.1016/j.engstruct.2016.01.012

Lüchinger, P. (1977). Ultimate Strength of Box-Griders in Reinforced Concrete under Torsion, Bendingand Shear. *Institut Für Baustatik Und Konstruktion*, *69*.

MacGregor, J. G., & Wight, J. K. (2005). *Reinforced Concrete: Mechanics and Design*.

Marti, P. (1985a). Basic Tools of Reinfored Concrete Beam Design. *ACI Structural Journal*,

82(1), 46–56.

Marti, P. (1985b). Truss Models in Detailing. *Concrete International*, *7*(12).

Martin, B., & Sanders, D. (2007). *Verification and implementation of strut-and-tie model in LRFD bridge design specifications*. *American Association of State Highway and Transportation Officials (AASHTO)*.

Mihaylov, B. I., Bentz, E. C., & Collins, M. P. (2013). Two-Parameter Kinematic Theory for Shear Behavior of Deep Beams. *ACI Structural Journal*, *110*(3), 34–56. https://doi.org/10.14359/51687180

Mohamed, K., Farghaly, A. S., & Benmokrane, B. (2016). Strut efficiency-based design for concrete deep beams reinforced with fiber-reinforced polymer bars. *ACI Structural Journal*, *113*(4), 791–800. https://doi.org/10.14359/51688476

Ramirez, J., & Breen, J. (1983). Proposed design procedures for shear and torsion in reinforced and prestressed concrete. *Center for Transportation Research*, (2), 270. Retrieved from http://library.ctr.utexas.edu/digitized/TexasArchive/phase1/248-4F-CTR.pdf

Reineck, K.-H. (2002). *Examples of the Design of Structural Concrete with Strut and Tie model*. *American Concrete Instutite*.

Richart, F. E. (1927). *An investigation of web stresses in reinforced concrete beams*. *Bulletin (University of Illinois (Urbana-Champaign campus).*

Ritter, W. (1899). Die Bauweise Hennebique. *Schweizerische Bauzeiung*, *33*(5), 42–61.

Russo, G., Venir, R., & Pauletta, M. (2006). Reinforced Concrete Corbels - Shear Strength Model and Design Formula. *ACI Structural Journal*, *103*(1). https://doi.org/10.14359/15080

Schlaich, J., Schäfer, K., & Jennewein, M. (1987). Toward a Consistent Design of Structural Concrete. *PCI Journal*, *32*(3), 74–150.

Shuraim, A. B., & El-Sayed, A. K. (2016). Experimental verification of strut and tie model for HSC deep beams without shear reinforcement. *Engineering Structures*, *117*, 71–85. https://doi.org/10.1016/j.engstruct.2016.03.002

Su, R. K. L., & Looi, D. T. W. (2016). Revisiting unreinforced strut efficiency factor. *ACI*

Structural Journal, *113*(2), 301–312. https://doi.org/10.14359/51688062

Talbot, F. (1909). *Tests of reinforced concrete beams: Resistance to web stresses*.

The International Federation for Structural Concrete. (2013). *fib Model Code for Concrete Structures 2010*.

Tseng, C. C., Hwang, S. J., & Lu, W. Y. (2017). Shear strength prediction of reinforced concrete deep beams with web openings. *ACI Structural Journal*, *114*(6), 1569–1579. https://doi.org/10.14359/51700950

Tuchscherer, R. G., Birrcher, D. B., & Bayrak, O. (2016). Reducing discrepancy between deep beam and sectional shear-strength predictions. *ACI Structural Journal*, *113*(1), 3–16. https://doi.org/10.14359/51688602

Tuchscherer, R. G., Birrcher, D. B., Williams, C. S., Deschenes, D. J., & Bayrak, O. (2014). Evaluation of existing strut-And-tie methods and recommended improvements. *ACI Structural Journal*, *111*(6), 1451–1460. https://doi.org/10.14359/51686926

Tuchscherer, R. G., Birrcher, D., & Bayrak, O. (2011). Strut-and-tie model design provisions. *PCI Journal*, *56*(1), 155–170. https://doi.org/10.15554/pcij.01012011.155.170

Williams, C., Deschenes, D., & Bayrak, O. (2012). Strut-and-Tie Model Design Examples for Bridges: Final Report, *7*, 258.